Applied Mathematics and Computation 456 (2023) 128122

Contents lists available at ScienceDirect

Applied Mathematics and Computation

journal homepage: www.elsevier.com/locate/amc

Modified SEIR epidemic model including asymptomatic and hospitalized cases with correct demographic evolution

Antonio Rafael Selva Castañeda[a,b], Erick Eduardo Ramirez-Torres[c], Luis Eugenio Valdés-García[d], Hilda María Morandeira-Padrón[e], Diana Sedal Yanez[f], Juan I. Montijano[a,*], Luis Enrique Bergues Cabrales[g,*]

[a] Instituto Universitario de Investigación de Matemáticas y Aplicaciones, Universidad de Zaragoza, Zaragoza, Spain
[b] Departamento de Telecomunicaciones, Facultad de Ingeniería en Telecomunicaciones, Informática y Biomédica, Universidad de Oriente, Santiago de Cuba, Cuba
[c] Departamento de Ingeniería Biomédica, Facultad de Ingeniería en Telecomunicaciones, Informática y Biomédica, Universidad de Oriente, Santiago de Cuba, Cuba
[d] Centro provincial de Higiene y Epidemiología, Santiago de Cuba, Cuba e Dirección Provincial de Salud pública, Santiago de Cuba, Cuba
[e] Dirección Provincial de Salud Pública, Santiago de Cuba, Cuba
[f] Facultad de Ciencias Sociales, Universidad de Oriente, Santiago de Cuba, Cuba
[g] Dirección de Ciencia e Innovación Tecnológica, Centro Nacional de Electromagnetismo Aplicado, Universidad de Oriente, Santiago de Cuba, Cuba

ARTICLE INFO

Article history:
Received 17 October 2022
Revised 5 May 2023
Accepted 15 May 2023
Available online 26 May 2023

Keywords:
Epidemics models
COVID-19
Mathematical modelling
Symptomatic cases
Asymptomatic cases
Hospitalized cases

ABSTRACT

The aim of this study is to propose a modified Susceptible-Exposed-Infectious-Removed (SEIR) model that describes the time behaviour of symptomatic, asymptomatic and hospitalized patients in an epidemic, taking into account the effect of the demographic evolution. Unlike most of the recent studies where a constant ratio of new individuals is considered, we consider a more correct assumption that the growth ratio is proportional to the total population, following a Logistic law, as is usual in population growth studies for humans and animals. An exhaustive theoretical study is carried out and the basic reproduction number R_0 is computed from the model equations. It is proved that if $R_0 < 1$ then the disease-free manifold is globally asymptotically stable, that is, the epidemics remits. Global and local stability of the equilibrium points is also studied. Numerical simulations are used to show the agreement between numerical results and theoretical properties. The model is fitted to experimental data corresponding to the pandemic evolution of COVID-19 in the Republic of Cuba, showing a proper behaviour of infected cases which let us think that can provide a correct estimation of asymptomatic cases. In conclusion, the model seems to be an adequate tool for the study and control of infectious diseases.

* Corresponding authors.
E-mail addresses: monti@unizar.es (J.I. Montijano), berguesc@yahoo.com (L.E.B. Cabrales).

https://doi.org/10.1016/j.amc.2023.128122

1. Introduction

Mathematical models have been a very important tool to study the evolution of epidemics since the early papers of Kermack and Mackendrick [1]. Since then, a lot of research has been developed in this area of knowledge [2]. Recently, the COVID-19 epidemic [3,4] has motivated new studies. This epidemic characterizes by the large number of pre-symptomatic and asymptomatic patients [5], which makes difficult to take effective governmental measures that control the disease [6], and the classical epidemic models have been extended so that more compartments of individuals (asymptomatic, hospitalized, etc.) have been taken into account [7,8].

In many studies of epidemics a constant population is assumed and neither new individuals (births) nor deaths are considered as in [9] where a multiregional model is considered to study the spatio temporal heterogeneity of an epidemic. In others it is included the variation of the population due to COVID-19 fatalities, but no births or natural deaths are considered. This is the case for example in [10] where the transmissibility of superspreaders individuals is studied. In [11], an individual reaction and governmental action based on some parameters of 1918 influenza pandemic is investigated. In that study, natural deaths are considered but no new individuals are introduced.

The assumption that the total population is constant and neither births nor deaths are taken into account is reasonable, for modeling epidemics in which the disease spreads rapidly through the population and eradicates in a short time. However, when the population growth or decrease is significant or the disease cause enough deaths, the assumption of constant population is not realistic. One of the most usual ways to include births and natural deaths is to assume that they are proportional to the total population. If $N(t)$ is the population, Λ is the birth ratio and μ is the death ratio, then

$$N' = (\Lambda - \mu)\left(1 - \frac{N}{N_{\max}}\right)N.$$

If $\Lambda - \mu > 0$, the population grows initially exponentially and it tends to the carrying capacity $N_{\max}$. If $\Lambda - \mu < 0$, the population decreases exponentially and if $\Lambda = \mu$ the population stays constant. If $N(0) = 0$, there can not be new individuals and the population stays zero forever (it is an equilibrium point).

Even though this is the most accepted model for population growth, and it had been used in previous models [12], in most of the recent studies of COVID-19, a constant ratio of birds has usually been assumed as in [13] where a theoretical study of a SAIRS compartmental model with vaccination is made. In [14] the dynamical behaviour of SIRS epidemic models were studied. In [15] the individual behavioural response due to information regarding proper precaution is analyzed, in [16] a model for evaluating a possibility to prevent, or delay, the local outbreaks of COVID-19 through restriction on travel form is implemented, in [17] it is analyzed how immigration, protection, death rate, exposure, cure rate and interaction of infected people with healthy people affect the population and in [18] it is proposed a hybrid computation technique to construct an epidemic model. These papers are a few of many others were it is assumed that the population evolves (in absence of infection) according to the equation

$$N' = \Lambda - \mu N,$$

that has a solution $N(t) = \left[N(0) - \frac{\Lambda}{\mu}\right]e^{-\mu t} + \frac{\Lambda}{\mu}$. With this model, if $N(0) < \Lambda/\mu$, the population always grows up (even if $N(0) = 0$) to the maximum value Λ/μ. This is not realistic if for example the birth ratio is smaller than the death ratio. This model represents in fact a population where a constant ratio of new people is introduced, as for example in [19] that studied an experiment with mice in laboratory.

In this paper we consider a model for the evolution of the epidemics that extends SEIR model by adding asymptomatic and hospitalized groups and includes terms for the demography evolution (births and deaths), in which the ratio of new individuals is proportional to the total population, according to a Logistic law. We analyze the differences in the behaviour of the solution with respect to models with constant growth ratio, that can be relevant. Thus, in the case of constant ratio it is usual the existence of a unique disease free equilibrium point and the origin is not an equilibrium point, whereas with ratio proportional to the total population, there can be a manifold of disease-free equilibrium points and the origin is always an equilibrium point.

In Section 2, we present the mathematical model with "correct" demographic term and analyze it theoretically. We prove the positivity of the solutions. Next,we obtain the basic reproductive number R_0 and we prove that the disease free manifold is globally asymptotically stable if $R_0 < 1$. Then, we analyze the stability of the equilibrium points of the system, showing its dependence with the value of R_0. In Section 3, we present some numerical simulations showing the dependency between numerical and theoretical results. In Section 4, we fit the parameters of the model with real data from Cuba showing that this model can reproduce the time behaviour of symptomatic and hospitalized cases. Then, we do the discussions of results and finally we present the conclusions.

2. Methods

2.1. Mathematical model

We consider an extended SEIR model with six states: susceptible ($S(t)$), exposed ($E(t)$), infected symptomatic ($I(t)$), infected asymptomatic ($A(t)$), hospitalized-isolated ($H(t)$) and recovered ($R(t)$) as shown in Fig. 1.

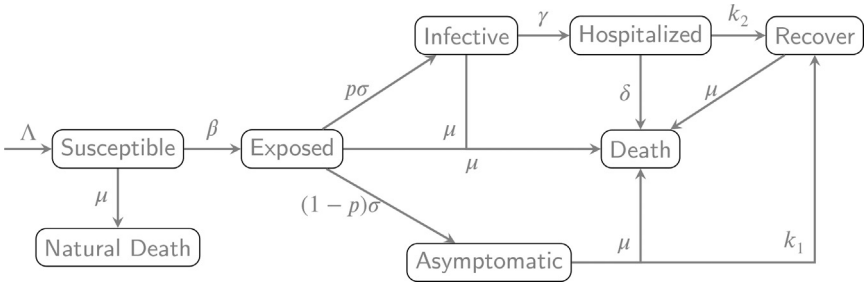

Fig. 1. Schematic representation for the formulation of the mathematical model for COVID-19 epidemic.

In the model, β (in days^{-1}) is the transmission rate, μ (in days^{-1}) the natural death rate, Λ (in days^{-1}) the birth rate, σ^{-1} (in days) the latent time, γ^{-1} (in days) the time between symptom onset to hospitalization, p the ratio between symptomatic and asymptomatic patients, k_1^{-1} (in days) the average recovery time of asymptomatic patients, k_2^{-1} (in days) the average recovery time of hospitalized patients and δ^{-1} (in days) is the average time that an hospitalized patient dies. Ramírez-Torres et al. [20] report that β changes over time and depends on transmission rate of SARCoV-2 strain, government measures, risk perception and social responsibility. For simplicity, we will assume that β is constant.

The relationships between these states are represented by the following system of ordinary differential equations

$$\begin{cases} \dfrac{dS}{dt} = \Lambda N - \dfrac{\beta S(I+A)}{N} - (\Lambda-\mu)\dfrac{N^2}{N_{max}} - \mu S \\ \dfrac{dE}{dt} = \dfrac{\beta S(I+A)}{N} - (\sigma+\mu)E \\ \dfrac{dI}{dt} = p\sigma E - (\gamma+\mu)I \\ \dfrac{dA}{dt} = (1-p)\sigma E - (k_1+\mu)A \\ \dfrac{dH}{dt} = \gamma I - k_2 H - (\delta+\mu)H \\ \dfrac{dR}{dt} = k_1 A + k_2 H - \mu R \end{cases} \tag{1}$$

where N is the total population, $N(t) = S(t) + E(t) + I(t) + A(t) + H(t) + R(t)$. Let us note that in this model, since we are considering births and deaths, the total population N changes with time.

We have not included in system (1) the evolution of the dead people since the analysis of the system can be done without it. Nevertheless, we can easily obtain the evolution of the dead people by adding the equation $D' = \mu N + \delta H$.

As mentioned in the introduction, unlike other models [7,8,13–18] where the ratio of new individuals is considered constant, we are considering it as ΛN, proportional to the total population, in agreement with the usual models of population growth. This can be more realistic than constant growth ratio, where, instead of the first equation of system (1) it would read

$$S' = \Lambda - \beta S\frac{(I+A)}{N} - \mu S.$$

Denoting $P = (S, E, I, A, H, R)^T$, the system can be formulated in compact form as

$$\frac{dP}{dt} = F(P).$$

The vector field $F(P)$ is well defined whenever $N \geq 0$. Moreover, variables of the differential system (1) have biological interpretation only when all of them are non negative. Thus, we will consider the domain

$$\mathcal{D} = \{P \in \mathbb{R}^6 \quad \text{such that } S, E, I, A, H, R \geq 0\}. \tag{2}$$

If $P \in \mathcal{D}$, we will write $P \geq 0$.

Note that the differential system is autonomous and we can assume, without loss of generality, that the initial time is $t_0 = 0$.

2.2. Positivity of the solution

Theorem 1. *The proposed system of differential Eq. (1) has a unique solution in $\mathcal{D}$. Moreover, if the initial condition of the system is such that all the variables are non-negative, $P(0) \in \mathcal{D}$, then all variables remain non negative over time. In other words, if the initial condition is in the positive hyperquadrant, the solution remains in this hyperquadrant.*

Proof. The vector field F is continuous in $\mathcal{D}$, and also differentiable (except at the zero point). The partial derivatives are uniformly bounded and therefore, the vector field is Lipschitz in the domain $\mathcal{D}$. This guarantees the existence and uniqueness of solution.

Now, to prove the positivity of the solutions, let us suppose that all variables are non negative at a certain time t^*. Obviously, $N(t^*) > 0$ since otherwise we would be in the null equilibrium solution. We will show that if at t^* a variable, let us name it generically $X(t^*)$, becomes zero, the first derivative that does not vanish at t^* must be positive, $X^{(k)}(t^*) > 0$ and therefore $X(t) > 0$ for $t \gtrsim t^*$.

First, if the S variable vanishes at t^* and $N(t^*) > 0$, then $S'(t^*) > 0$ and necessarily $S(t)$ is positive for $t \geq t^*$.

It is observed that if $E(t^*) = I(t^*) = A(t^*) = 0$, their derivatives also vanish at that point and therefore, it would be $E(t) = I(t) = A(t) = 0$ for all t (equilibrium point of this subsystem, regardless of the values that S, H, R have). Furthermore, in this case, $H' = -(\delta + k_2 + \mu)H$ and $R' = k_2 H - \mu R$, consequently both are non negative for all $t > t^*$.

If $E(t^*) = 0$, then

$$E'(t^*) = \beta \frac{S(t^*)(I(t^*) + A(t^*))}{N(t^*)} - (\sigma + \mu)E(t^*),$$

$$E''(t^*) = S'(t^*)\beta \frac{(I(t^*) + A(t^*))}{N(t^*)} + (I'(t^*) + A'(t^*))\beta \frac{S(t^*)}{N(t^*)} - \beta S(t^*)(I(t^*) + A(t^*))\frac{N'(t^*)}{N(t^*)^2} - (\sigma + \mu)E'(t^*).$$

If $S(t^*)(I(t^*) + A(t^*)) > 0$, then $E'(t^*) > 0$. If $S(t^*) = 0$ but $(I(t^*) + A(t^*)) > 0$ then $E'(t^*) = 0$, $S'(t^*) > 0$ and $E''(t^*) > 0$. If $(I(t^*) + A(t^*)) = 0$, then $E(t^*) = I(t^*) = A(t^*) = 0$. In conclusion, $E(t) > 0$ for $t \gtrsim t^*$.

If this analysis is performed with the other variables and proceeding in a similar way to the $E(t^*)$ case, it is proved that these variables remain non negative at $t \geq t^*$ if they cancel out at t^*. □

The positivity of the solutions can also be proved in a similar way in the case of considering a constant growth ratio.

2.3. Stability of disease free manifold

If $E = I = A = 0$, the system (1) reduces to

$$S' = \Lambda(S + H + R) - \mu S - (\Lambda - \mu)\frac{(S + H + R)^2}{N_{max}}.$$

Note that by the uniqueness of solution of system (1), if some of $E(0), I(0)$ or $A(0)$ are not zero there cannot be any time t at witch these three variables vanish simultaneously.

The contagion-free manifold will be defined as the set

$$CFM = \{(S, 0, 0, 0, H, R)^T, S, H, R \geq 0\}, \tag{3}$$

and as we have observed, it is an invariant manifold.

Let us consider a point Q^* in the *CFM*. The Jacobian matrix of the vector field at Q^* can be written as follows

$$J = \begin{pmatrix} \mathcal{A} & \mathcal{B} & \mathcal{B} - \frac{\beta S^*}{N^*} & \mathcal{B} - \frac{\beta S^*}{N^*} & \mathcal{B} & \mathcal{B} \\ 0 & -(\sigma + \mu) & \frac{\beta S^*}{N^*} & \frac{\beta S^*}{N^*} & 0 & 0 \\ 0 & p\sigma & -(\gamma + \mu) & 0 & 0 & 0 \\ 0 & (1-p)\sigma & 0 & -(k_1 + \mu) & 0 & 0 \\ 0 & 0 & \gamma & 0 & -(k_2 + \delta + \mu) & 0 \\ 0 & 0 & 0 & k_1 & k_2 & -\mu \end{pmatrix},$$

with

$$\mathcal{A} = (\Lambda - \mu)\left[1 - 2\frac{N^*}{N_{\max}}\right], \ \mathcal{B} = \Lambda - 2(\Lambda - \mu)\frac{N^*}{N_{\max}} \text{ and } N^* = S^* + H^* + R^*.$$

This matrix has the eigenvalue $\frac{(\Lambda-\mu)(N_{\max}-2N^*)}{N_{\max}}$, and its associated eigenvector is $(1, 0, \ldots, 0)^T$. This means that the component of the fundamental solution associated with the eigenvalue $\frac{(\Lambda-\mu)(N_{\max}-2N^*)}{N_{\max}}$ only affects the first variable S. The behaviour of the other variables will depend on the remaining five eigenvalues. The eigenvalue $-\mu$ has the eigenvector $(-1, \ldots, 0, 1)^T$. The component associated with the eigenvalue $-\mu$ affects the variables S and R. Another eigenvalue is

$-(k_2+\delta+\mu)$, whose eigenvector is $\left(\frac{\delta(\Lambda N_{\max}-2(\Lambda-\mu)N^*)}{k_2(N_{\max}(k_2+\delta+\Lambda)-2(\Lambda-\mu)N^*)}, 0, 0, 0, -\frac{k_2+\delta}{k_2}, 1\right)^T$. The component of the solution associated with this eigenvalue affects the variables S, H and R. This means that the behaviour of the variables E, I and A around the point Q^* depends only on the three remaining eigenvalues.

The remaining three eigenvalues are those of the main submatrix of J of dimension 3 obtained by eliminating the first and the last two rows and columns. The trace of this submatrix is clearly negative and a necessary condition for the equilibrium point not to be unstable is that its determinant is negative, that is,

$$\beta\sigma\left[\frac{S^*}{S^*+H^*+R^*}\right]((1-p)(\gamma+\mu)+p(k_1+\mu))-(k_1+\mu)(\gamma+\mu)(\mu+\sigma)<0, \tag{4}$$

that can be written in the form

$$\frac{S^*}{S^*+H^*+R^*}R_0<1, \tag{5}$$

with

$$R_0=\frac{\beta(k_1p\sigma+p\mu\sigma+(1-p)(\gamma+\mu)\sigma)}{(\gamma+\mu)(k_1+\mu)(\mu+\sigma)}. \tag{6}$$

Applying the Routh-Hurwitz criterion to the submatrix of J associated to the variables E, I, A, we obtain that the eigenvalues of this submatrix have negative real part if and only if Eq. (5) is satisfied. If we impose the condition to be satisfied for all points Q^* in the *CFM*, then it must be $R_0<1$, that is, the *CFM* is locally stable if $R_0<1$.

If we apply the new generation matrix method reported in [21,22] at a point Q^* in the *CFM*, we obtain the matrices

$$\mathcal{F}=\begin{pmatrix}0 & \frac{\beta S^*}{S^*+H^*+R^*} & \frac{\beta S^*}{S^*+H^*+R^*}\\ 0 & 0 & 0\\ 0 & 0 & 0\end{pmatrix},$$

$$\mathcal{V}^{-1}=\begin{pmatrix}\frac{1}{(\mu+\sigma)} & 0 & 0\\ \frac{\sigma p(k_1+\mu)}{(k_1+\mu)(\gamma+\mu)(\mu+\sigma)} & \frac{1}{(\gamma+\mu)} & 0\\ -\frac{(p-1)\sigma}{(k_1+\mu)(\mu+\sigma)} & 0 & \frac{1}{(k_1+\mu)}\end{pmatrix},$$

The basic reproduction number is given by the maximum absolute value of the eigenvalues of the matrix $\mathcal{F}\mathcal{V}^{-1}$, that is, its spectral radius. In this case we obtain the expression Eq. (5) and if we consider the maximum value in S^*, H^*, R^*, that is in the whole *CFM*, we obtain R_0 in Eq. (6) as the basic reproductive number.

Let's analyze when this variety is globally asymptotically stable, that is, under what conditions on the parameters $E(t)\to 0$, $I(t)\to 0$, $A(t)\to 0$ regardless of the values taken by S, H, R. Consider the equations associated with E, I and A, given by

$$\begin{cases}\frac{dE}{dt}=\frac{\beta S(I+A)}{N}-(\sigma+\mu)E\\ \frac{dI}{dt}=p\sigma E-(\gamma+\mu)I\\ \frac{dA}{dt}=(1-p)\sigma E-(k_1+\mu)A\end{cases}. \tag{7}$$

These three equations can be rewritten as

$$y'=My-v, \tag{8}$$

where

$$y=(E,I,A)^T, \tag{9}$$

and

$$M=\begin{pmatrix}-(\sigma+\mu) & \beta & \beta\\ p\sigma & -(\gamma+\mu) & 0\\ (1-p)\sigma & 0 & -(k_1+\mu)\end{pmatrix}, v=\begin{pmatrix}g(t)\\ 0\\ 0\end{pmatrix}, \tag{10}$$

with

$$g(t)=\beta(I(t)+A(t))\left(1-\frac{S(t)}{N(t)}\right).$$

It is clear that $g(t)\geq 0\forall t$.

In order to prove the global stability, we will make use of the following comparison Theorem

Theorem 2. *Let us suppose that*

- $x = (x_1 \ldots, x_n)^T$ *is a vector of* R^n.
- $f(t, x)$ *is a Lipschitz continuous function in* $[t_0, \infty] \times \mathcal{E}$, $\mathcal{E}$ *open subset of* R^n, *which is quasi monotonic, non decreasing, that is, each component of* $f_i(t, x_1, \ldots, x_n)$ *is monotonic non decreasing in the variables* x_j *with* $j \neq i$.
- $y(t)$ *is a differentiable function in R with* $y(t) \in \mathcal{E}$.
- $z(t)$ *is a solution of* $z' = f(t, z)$.
- $y_i(t_0) \leq z_i(t_0)$ $\forall i$.
- $y_i'(t) \leq f_i(t, y)$ $\forall i$ *and* $\forall y \in \mathcal{E}$.

Then $y_i(t) \leq z_i(t), i = 1, 2, \ldots, n \forall t$.

Proof. This result is a particular case of Corollary 1.7.1 in [23] and also of comparison Theorems in [24]. □

Then, we can state the following stability result.

Theorem 3. *If* $R_0 < 1$, *then* $E(t) \to 0$, $I(t) \to 0$ *and* $A(t) \to 0$ *and disease free manifold is globally stable.*

Proof. Let us apply Theorem 2 with $y(t)$ the solution of (8) and $f(t, y) = My$. It is clear that My is a quasi monotonic non decreasing function since the non diagonal elements of M are non negative. It is also clear that $y_i' \leq f_i(t, y)$ because $g(t)$ is greater or equal to zero. Taking $y(0) = z(0)$ we conclude that $y_i(t) \leq z_i(t)$ for all $t > 0$. Now let us note that the matrix M is in fact the submatrix of J obtained by eliminating the first and the last two rows and columns and putting $H^* = R^* = 0$. Then if $R_0 < 1$, the three eigenvalues of M have real part smaller than 0 and $z(t) \to 0$. Consequently, $y(t) \to 0$ (note that $y_i(t) \geq 0$). This proves the global stability of the contagious free manifold. Additionally, if we include in Eq. (8) the equation (linear) of system (1) corresponding to $H(t)$, with the same reasoning we obtain that $H(t) \to 0$, and the disease free contagious manifold is globally asymptotically stable. □

Remark 1. The above results are also true for the case of considering a constant growth ratio. There is however a relevant difference in the evolution of the susceptible population. Whereas in the case of constant growth ratio S always tends to its maximum value Λ/μ (S tends to be equal to N if $\mu > 0$), when the growth ratio is proportional to the total population, S tends to zero if $\Lambda < \mu$, or tends to a constant if $\Lambda \geq \mu$, as we will see in the next subsections.

2.4. Stability of the equilibrium points

2.4.1. Case $\Lambda > \mu$

If parameters of the system (1) are all positive, this system of equations has two critical points, $P_1^* = (N_{\max}, 0, 0, 0, 0, 0)^T$ and $P_2^* = (0, 0, 0, 0, 0, 0)^T$. Moreover, denoting

$$\alpha = \frac{\delta\gamma\mu p\sigma(R_0 - 1)}{R_0(\Lambda - \mu)[(\gamma + \mu)(\mu + \sigma)(\delta + k_2 + \mu) - \delta\gamma p\sigma]}, \tag{11}$$

when $R_0 > 1$ and $0 \leq \alpha \leq 1$ there exist a third equilibrium point $P_3^* = (S^*, E^*, I^*, A^*, H^*, R^*)^T$ given by

$$S^* = \frac{N^*}{R_0}, \tag{12}$$

$$E^* = \frac{(\gamma + \mu)(k_2 + \delta + \mu)(\Lambda - \mu)(\alpha(1 - \alpha)N_{\max})}{p\sigma\gamma\delta}, \tag{13}$$

$$I^* = \frac{(k_2 + \delta + \mu)(\Lambda - \mu)(\alpha(1 - \alpha)N_{\max})}{\gamma\delta}, \tag{14}$$

$$A^* = \frac{(1 - p)(\gamma + \mu)(k_2 + \delta + \mu)(\Lambda - \mu)(\alpha(1 - \alpha)N_{\max})}{p\gamma\delta(k_1 + \mu)}, \tag{15}$$

$$H^* = \frac{(\Lambda - \mu)(\alpha(1 - \alpha)N_{\max})}{\delta}, \tag{16}$$

$$R^* = \frac{(\Lambda - \mu)(\alpha(1 - \alpha)N_{\max})}{\mu\delta}\left[\frac{k_1(1 - p)(\gamma + \mu)(k_2 + \delta + \mu)}{p\gamma(k_1 + \mu)} + k_2\right], \tag{17}$$

and

$$N^* = N_{\max}(1 - \alpha). \tag{18}$$

Concerning P_1^*, the Jacobian matrix of the system is

$$J = \begin{pmatrix} -(\Lambda-\mu) & -(\Lambda-2\mu) & -(\Lambda-2\mu)-\beta & -(\Lambda-2\mu)-\beta & -(\Lambda-2\mu) & -(\Lambda-2\mu) \\ 0 & -(\mu+\sigma) & \beta & \beta & 0 & 0 \\ 0 & p\sigma & -(\gamma+\mu) & 0 & 0 & 0 \\ 0 & (1-p)\sigma & 0 & -(k_1+\mu) & 0 & 0 \\ 0 & 0 & \gamma & 0 & -(\delta+k_2+\mu) & 0 \\ 0 & 0 & 0 & k_1 & \delta & -\mu \end{pmatrix}. \tag{19}$$

This matrix has the eigenvalue $-(\Lambda-\mu)$ and its associated eigenvector is $(1,0,\ldots,0,0)$. This means that the component of the fundamental solution associated with the eigenvalue $-(\Lambda-\mu)$ affects the variables S. The behaviour of the other variables will depend on the remaining five eigenvalues. The eigenvalue $-\mu$ has the eigenvector $(-1,\ldots,0,1)^T$. The component associated with the eigenvalue $-\mu$ affects the variables S and R. Another eigenvalue is $-(\delta+\delta+\mu)$, and has the eigenvector $(-\frac{k_2(\Lambda-\mu)}{\delta(k_2+\delta+2\mu-\Lambda)},0,0,0,-\frac{k_2+\delta}{\delta},1)^T$. This means that the component of the fundamental solution associated with the eigenvalue $-(\delta+\delta+\mu)$ affects the variables S, H and R. This means that the behaviour of the variables E, I and A around the point P_1^* depends only on the three remaining eigenvalues.

The remaining three eigenvalues are those of the main submatrix of J of dimension 3 obtained by eliminating the first and the last two rows and columns. The trace of this submatrix is clearly negative and a necessary condition for the equilibrium point not to be unstable is that its determinant is negative, that is,

$$\beta\sigma((1-p)(\gamma+\mu)+p(k_1+\mu))-(k_1+\mu)(\gamma+\mu)(\mu+\sigma)<0, \tag{20}$$

There we concluded that the system (1) is stable if three eigenvalues of submatrix J have negative real part and this is fulfilled if and only if $R_0<1$, with R_0 given by Eq. (6). This value coincides with the one obtained by the new generation matrix method [21,22].

For equilibrium point P_2^* the Jacobian matrix of the system has some components with the term

$$\frac{\beta S(S+E+A+H+R)}{(S+E+I+A+H+R)^2},$$

which is not continuous when variables tend to zero. Therefore, we cannot use linearization to study the local stability of the origin.

We will obtain next some conditions on the parameters of the model and the initial conditions for which the population tends globally to the equilibrium point P_1^* and the origin can not be stable.

Theorem 4. *If $\Lambda>\mu$ and $R_0<1$, there exist a constant K such that if $N(0)>K$, then the total population $N(t)$ tends to $N_{\max}$ when $t\to\infty$, that is, P_1^* is globally asymptotically stable.*

Proof. Let us consider the linear system

$$\begin{cases} \dfrac{d\hat{E}}{dt} = \beta\hat{I}+\beta\hat{A}-(\sigma+\mu)\hat{E} \\ \dfrac{d\hat{I}}{dt} = p\sigma\hat{E}-(\gamma+\mu)\hat{I} \\ \dfrac{d\hat{A}}{dt} = (1-p)\sigma\hat{E}-(k_1+\mu)\hat{A} \\ \dfrac{d\hat{H}}{dt} = \gamma\hat{I}-k_2\hat{H}-(\delta+\mu)\hat{H} \end{cases}. \tag{21}$$

whose general solution has the form

$$\hat{P}(t) = C_1\vec{v_1}e^{\lambda_1 t}+C_2\vec{v_2}e^{\lambda_2 t}+C_3\vec{v_3}e^{\lambda_3 t}+C_4\vec{v_4}e^{\lambda_4 t}, \tag{22}$$

where $\lambda_1,\lambda_2,\lambda_3$ are the eigenvalues of the matrix M in (10), $\lambda_4=-(k_2+\delta+\mu)$ and v_i are the corresponding eigenvectors. Proceeding as in Theorem 3, the components E,I,A,H of the solution of system (1) are upper bounded by the ones of Eq. (21) and in particular

$$H(t)\le\hat{H}(t)=B_1e^{\lambda_1 t}+B_2e^{\lambda_2 t}+B_3e^{\lambda_3 t}+B_4e^{\lambda_4 t}. \tag{23}$$

where B_i are constants that depend on the eigenvectors v_i and the initial conditions.

Denoting $u=max_i Re\lambda_i$, if $R_0<1$, then $u<0$, $H(t)$ goes to zero and there exists a constant B such that

$$H(t)\le Be^{ut}, u<0, \tag{24}$$

Adding the equations of system (1), we get

$$dN/dt = (\Lambda - \mu)\left[1 - \frac{N}{N_{\max}}\right]N - \delta H. \tag{25}$$

If the bound (24) is substituted in Eq. (25) we get

$$\frac{dN}{dt} \geq (\Lambda - \mu)\left[1 - \frac{N}{N_{\max}}\right]N - \delta B e^{ut}. \tag{26}$$

If there exist a constant $\hat{N} < N_{\max}$ such that

$$N(t) \leq \hat{N} < N_{\max}, \forall t, \tag{27}$$

then

$$\frac{dN}{dt} \geq (\Lambda - \mu)\alpha N - \delta B e^{ut}, \tag{28}$$

where

$$\alpha = \left[1 - \frac{\hat{N}}{N_{\max}}\right], \tag{29}$$

which implies

$$N(t) \geq \left[N(0) - \frac{\delta B}{u - (\Lambda - \mu)\alpha}\right]e^{(\Lambda-\mu)\alpha t} + \frac{\delta B}{u - (\Lambda - \mu)\alpha}e^{ut}, \tag{30}$$

and since $\Lambda - \mu > 0$, if $N(0) > \frac{\delta B}{u-(\Lambda-\mu)\alpha}$, $N(t)$ would tend to infinity, which contradicts that $N(t) \leq \hat{N}$.

Note that the constant B depends on the initial conditions $E(0), I(0), A(0), H(0)$ and therefore $S(0) + R(0)$ must be large enough with respect to the other initial conditions. □

The above result let us know that the population grows with time if $R_0 < 1$ and the initial population is large enough. We will see next that under a little more restrictive condition on R_0, the total population grows with time whatever the initial population is.

Theorem 5. *If* $\Lambda - \mu > 0$ *and*

$$\hat{R}_0 = \frac{\beta\sigma[k_1 p + (1-p)\gamma]}{\gamma k_1 \sigma} < 1, \tag{31}$$

then $S(t)$ *tends to* $N_{\max}$ *when* $t \to \infty$.

Proof. From system (1) we have

$$R'(t) = k_1 A + K_2 H - \mu R(t) \geq -\mu R(t), \tag{32}$$

There exist a point t_0 for which $R(t_0) > 0$ (note that if $R(0) = 0$, from Theorem 1 $R(t) > 0$ in a neighbourhood of 0). Then, we have the bound

$$R(t) \geq R(t_0)e^{-\mu t}, \forall t \geq t_0, \tag{33}$$

Now, note that R_0 is a decreasing monotone function with respect to μ. Therefore $R_0 \leq \hat{R}_0 < 1$ for any $\mu > 0$ and Theorem 3 applies. There exist a constant K such that

$$I(t) + A(t) \leq Ke^{ut}, \forall t \geq t_0, \tag{34}$$

u being the maximum real part of the eigenvalues of matrix M in Eq. (10). Let us suppose again that $N(t) \leq \hat{N} < N_{\max}$. Using Eq. (33) and Eq. (34) in the first equation of system (1), we obtain

$$\begin{aligned} S'(t) &\geq (\Lambda - \mu)\alpha S - S\beta\frac{I + A}{I + A + R}, \\ S'(t) &\geq S\left[(\Lambda - \mu)\alpha - \beta\frac{Ke^{ut}}{Ke^{ut} + R(t_0)e^{-\mu t}}\right], \forall t \geq t_0. \end{aligned} \tag{35}$$

Since $\hat{R}_0 < 1$, then $u < -\mu$ and consequently

$$\frac{Ke^{ut}}{Ke^{ut} + R(t_0)e^{-\mu t}} \to 0. \tag{36}$$

Table 1
Parameters for numerical study of stability of system (1).

Parameters	Values
N	10000
$N_{\max}$	100000
p	0.5500
k_1^{-1} (days)	14.0000
σ^{-1} (days)	5.1000
k_2^{-1} (days)	20.0000
δ^{-1} (days)	15.0000
γ^{-1} (days)	3.0000
β	1.000
R_0	6.7824

There will exist a time t^* and a positive constant C such that

$$(\Lambda-\mu)\alpha-\beta\frac{Ke^{ut}}{Ke^{ut}+R(t_0)e^{-\mu t}}\geq C>0,\forall t\geq t^*. \tag{37}$$

Therefore,

$$S'(t)\geq CS(t),\forall t\geq t^*, \tag{38}$$

which would imply that $S(t)$ tends to infinity. This contradicts that $N(t)<=\hat{N}$ and therefore $N(t)$ tends to $N_{\max}$. This means that $S(t)$ tends to $N_{\max}$.

Recall that $u=\max Re\lambda_i$, where $\lambda_1,\lambda_2,\lambda_3$ are the eigenvalues of M and $\lambda_4=-(k_1+\delta+\mu)<\mu$. Then, the condition $u<-\mu$ is equivalent to say that the real parts of the eigenvalues of M are smaller than $-\mu$. But, the eigenvalues of M are precisely the eigenvalues of the matrix M with $\mu=0$ minus μ, that is

$\lambda_i(\mu)=\lambda_i(\mu=0)-\mu$, which implies that $u<-\mu$ if $Re\lambda_i(mu=0)<0$.

The eigenvalues $\lambda_i(\mu=0)$ have real part smaller than 0 if and only if $\hat{R}_0=R_0(\mu=0)<1$ and this proves the theorem. □

Remark 2. If a constant growth ratio is considered, it can be proved that if $R_0<1$, the total population tends to Λ/μ whatever the values of Λ and μ are.

Concerning the critical points P_2^* and P_3^*, a theoretical analysis is complex and we have not been able to prove their stability. However, an exhaustive numerical study has led us to the following conclusion.

Conjecture 1. *If* $R_0>1$

- *And* $\alpha\in(0,1)$, *then* $P(t)\to P_3^*$.
- *And* $\alpha\geq 1$, *then* $P(t)\to P_2^*$.

In order to show numerically these results, an experimental simulation is presented here for three different initial conditions $P_{11}^*(8520,1000,100,80,200,0)$, $P_{22}^*(6310,500,50,40,100,0)$, and $P_{33}^*(3740,2000,200,160,400,1500)$. We calculate numerically the phase portraits of the system (1) and found that all trajectories end at the conjectured equilibrium points for the parameters shown in Table 1. These phase portraits (Appendix A) suggest that the system (1) can be asymptotically stable.

2.4.2. Case $\Lambda<\mu$

First, by adding the equations of system (1), we get

$$\mathrm{d}N/\mathrm{d}t=(\Lambda-\mu)\left[1-\frac{N}{N_{\max}}\right]N-\delta H.$$

If parameters of the system (1) are all positive, this system of equations has two critical point $P_1^*=(N_{\max},0,0,0,0,0)^T$ and $P_2^*=(0,0,0,0,0,0)^T$. For P_1^* the jacobian matrix of the system (1) is calculated in Section 2.4.1 by Eq. (19). For this equilibrium point at least one of the eigenvalues has a positive real part therefore, the system is unstable. The Jacobian matrix of the system for point P_2^* is not continuous at zero and we can not use linearization to study the local stability. Nevertheless it is possible to see that this point is globally stable.

Theorem 6 *(Global stability of* P_2^**). If at* $t=0$, *all variables are non negative and* $\Lambda<\mu$, *they tend to zero when* $t\to\infty$.

Proof. As $\Lambda<\mu$, if $H\geq 0$, the total population N decreases and tends to zero as t tends to infinity. By Theorem 1, $H(t)\geq 0$, which implies that $N'(t)\leq(\Lambda-\mu)\left[1-\frac{N}{N_{\max}}\right]N$. Therefore, $N(t)\to 0$ when $t\to\infty$, and since all variables are non negative, they must tend to zero. □

This result confirms that the proposed model is consistent with the biological system, because all variables in system (1) tend to zero, but does not provide information on the epidemic behaviour. In practice, the values of Λ and μ are small. If $\Lambda < \mu$, total population will tend to die after a long time, but what we want to know is if the epidemic remits (E, I, A, H tend to zero) in a reasonable period of time, leaving only the S and R populations, or the epidemic becomes endemic (E, I, A, H tend to zero slowly, at a speed similar to that of S), or if the epidemic affects the entire population (S, E, I, A, H tend to zero in a reasonable period of time). According to Theorem 3 if the basic reproduction number R_0 is smaller than 1, the infection remits exponentially at least as e^{ut}, u being the largest real part of matrix M in (8). If $u < -\mu$, the infection remits faster than the natural dead speed, that is, the disease remits (see (35) and use (36)). Nevertheless, if u is close to $-\mu$, the infection can stay active for a long time. Additional information can be obtained by studying the cases $\Lambda = \mu$ and $\Lambda = \mu = 0$.

Note that if we compute R_0 by applying the new generation matrix methods reported in [21,22] at the null equilibrium point we obtain again the value (6).

2.4.3. Case $\Lambda = \mu$

In this case, the total population satisfies

$$dN/dt = -\delta H,$$

which implies that $N(t)$ is non negative and decreases if $H \geq 0$. This means that $N(t)$ has a limit $N^* \geq 0$ when $t \to \infty$.

If parameters of the system (1) are positive, any point $P^* = (S^*, 0, 0, 0, 0, 0)^T$ is an equilibrium point. The Jacobian matrix of the system at the equilibrium point (limit of the Jacobian matrix at a point P when it tends to P^*) with $S^* > 0$ can be written as follows

$$J = \begin{pmatrix} 0 & 0 & -\beta & -\beta & 0 & 0 \\ 0 & -(\sigma+\mu) & \beta & \beta & 0 & 0 \\ 0 & p\sigma & -(\gamma+\mu) & 0 & 0 & 0 \\ 0 & (1-p)\sigma & 0 & -(k_1+\mu) & 0 & 0 \\ 0 & 0 & \gamma & 0 & -(k_2+\delta+\mu) & 0 \\ 0 & 0 & 0 & k_1 & k_2 & -\mu \end{pmatrix}.$$

This matrix has the eigenvalue 0, the eigenvector associated with this eigenvalue is $(1, 0, \ldots, 0)^T$. This means that the component of the fundamental solution associated with the eigenvalue 0 only affects the first variable S. The behaviour of other variables will depend on the remaining five eigenvalues. The eigenvalue $-(k_2+\delta+\mu)$ has the eigenvector $(0, 0, 0, 0, -\frac{k_2+\delta}{\delta}, 1)^T$. The component associated with the eigenvalue $-(k_2+\delta+\mu)$ only affects the variables H and R. Another eigenvalue is $-\mu$, whose eigenvector is $(0, 0, 0, \ldots, 1)^T$. The component of the solution associated with this eigenvalue only affect the variable R. This means that the behaviour of the variables E, I and A depends on the three remaining eigenvalues.

The remaining three eigenvalues are those of the main submatrix of dimension 3 obtained by eliminating the first and the last two rows and columns. But this submatrix is the same as the one studied in Section 2.3, but with $H^* = R^* = 0$. There we concluded that their three eigenvalues have negative real part ($u < 0$) if and only if $R_0 < 1$, with R_0 given by Eq (6). This value coincides with that obtained by the new generation matrix method [21,22].

If $R_0 > 1$, all the equilibrium points (except possibly the zero point) are unstable. If $R_0 < 1$, since the Jacobian matrix has an eigenvalue zero, we can not conclude their stability.

Note that at the origin the Jacobian matrix of the system (1) is not defined (there is no limit when all variables tend to zero) and the linearization theorem cannot be applied. The following results give some insight about their stability.

Lemma 1. *Let $f(t)$ be a twice differentiable function, with a second derivative bounded at $[0, \infty)$. If $\lim_{t\to\infty} |f(t)| = f^* < \infty$ then $\lim_{t\to\infty} f'(t) = 0$.*

Proof. First, if $f'(t)$ does not vanish when $t \to \infty$, we can ensure that for large t $\left|f'(t)\right| > M$ that implies that $f(t)$ cannot be bounded. If $f'(t)$ has no limit, the upper and lower limit are real numbers, not equal to each other and there exist a constant α such that,

$$\liminf_{t\to\infty} f'(t) < \alpha < \limsup_{t\to\infty} f'(t)$$

In addition, $\liminf f'(t) \cdot \limsup f'(t) \leq 0$ because otherwise we ensure that $\left|f'(t)\right| > M$ for large enough t. From the definition of upper limit, there exists a sequence of values of $f(t)$ approaching the upper limit, and another sequence of values of $f(t)$ approaching the lower limit. Let us suppose that $\alpha > 0$ (the case $\alpha < 0$ is similar). There exist infinite sequences $\{t_k\}$

and $\{s_k\}$, such that,

$$\begin{cases} k = 1, 2, 3, 4 \ldots. \\ t_1 < s_1 < t_2 < s_2 < \ldots \to \infty \\ f'(t_k) > \alpha \\ f'(s_k) = \dfrac{\alpha}{2} \\ f'(t) \geq \dfrac{\alpha}{2} t \in [t_k, s_k]. \end{cases}$$

The second derivative is bounded by a positive constant K and applying the mean value theorem, we obtain

$$\frac{\alpha}{2} \leq \left| f'(t_k) - f'(s_k) \right| \leq K|t_k - s_k|,$$

therefore,

$$|t_k - s_k| \geq \frac{\alpha}{2K}.$$

Applying again the mean value theorem, for some $c \in (t_k, s_k)$

$$|f(t_k) - f(s_k)| = f'(c)|t_k - s_k| \geq \frac{\alpha^2}{4K}.$$

But this inequality contradicts the Cauchy condition, which states that

$$\lim_{\substack{t \to \infty \\ s > t}} |f(t) - f(s)| = 0,$$

and consequently,

$$\liminf_{t \to \infty} f'(t) = 0, \limsup_{t \to \infty} f'(t) = 0. \qquad \square$$

Lemma 2. *If the initial conditions are non negative, $P(0) \in \mathcal{D}$, and $\Lambda = \mu$, then $S(t)$, $E(t)$, $I(t)$, $A(t)$, $H(t), R(t)$ are bounded and have two bounded derivatives in $[t_0, \infty]$.*

Proof. It is a direct consequence of the form of system (1), the boundedness of N and Theorem 3. $\square$

Lemma 3. *If the initial conditions are non negative, $P(0) \in \mathcal{D}$, and $\Lambda = \mu$, then $N(t)$ has a limit $N^* \geq 0$ when $t \to \infty$ and $\lim_{t \to \infty} N'(t) = 0$.*

Proof. It is consequence of Lemma 1. $\square$

Lemma 4. *If $\Lambda = \mu \neq 0$ and $\lim_{t \to \infty} S(t) = 0$, then $\lim_{t \to \infty} N(t) = 0$ and all variables tend to zero when t tends to infinity.*

Proof. From Lemma 1, if $S(t)$ tends to zero, then $S'(t)$ tends to zero, and using the first equation in (1), $N(t)$ tends to zero. $\square$

Theorem 7. *Let us consider the system (1) with initial condition $P(0) \in \mathcal{D}$, and $\Lambda = \mu \neq 0$. Then*

- *Any solution tends to an equilibrium point $(S^*, 0, 0, 0, 0)$ when $t \to \infty$.*
- *If (31) is satisfied, then any solution whose initial condition does not vanish tends to an equilibrium point with $S^* > 0$. The origin is unstable.*
- *If $R_0 > 1$, then $N(t) \to 0$ when $t \to \infty$. The origin (equilibrium point with $S^* = 0$) is globally asymptotically stable.*
- *If $R_0 < 1$, then the equilibrium points P^* with $S^* > 0$ are stable.*

Proof. According to Lemma 3, $N(t)$ has limit $N^* \geq 0$ and its derivative tends to zero when t tends to infinity. Therefore, $H(t)$ also tends to zero, and since its second derivative is bounded at $[t_0, \infty]$, we can ensure that $H'(t) \to 0$. This implies that $I(t)$ tends to zero and therefore also $I'(t) \to 0$. From the third of the differential equations, $E(t)$ should tend to zero, so that $E'(t) \to 0$, and hence either $S(t) \to 0$, which implies (by Lemma 4) that the solution tends to the origin, or $A(t) \to 0$. In this case, $E(t), I(t), A(t)$ and $H(t) \to 0$, so $R(t) \to 0$. This implies that the solution tends to an equilibrium point P^*.

From the first equation of system (1) it is clear that

$$S' \geq \Lambda R - \beta(I + A). \tag{39}$$

Proceeding as in Theorem 5 and using the bounds (33) and (34), we obtain

$$S' \geq R(t_0)e^{-\mu t}\left[\Lambda - \beta \frac{ke^{ut}}{R(t_0)e^{-\mu t}}\right], \tag{40}$$

where u is again the maximum real part of the eigenvalues of the matrix M in (10).

If Eq. (31) is satisfied, then $|u| > |\mu|$ and

$$\frac{ke^{ut}}{R(t_0)e^{-\mu t}} \to 0. \tag{41}$$

There will exist a time t^* such that

$$\left[\Lambda - \beta \frac{ke^{ut}}{R(t_0)e^{-\mu t}}\right] \geq D > 0, \forall t \geq t^*, \tag{42}$$

Therefore, for $t > t^*$, $S(t)$ is an increasing and upper bounded function that must have a limit $S^* > 0$. If $R_0 > 1$, then all the equilibrium points with $S^* > 0$ are unstable.

To prove the stability of P^*, let us see that there exists $\epsilon > 0$ for $\delta > 0$, such that if $\| P(0) - P^* \| < \epsilon$, then $\| P(t) - P^* \| < \delta$, $\forall t$. Let us consider the maximum norm and $\| P(0) - P^* \| < \epsilon$. We must see that $\| S(t) - S^* \| < \delta$, and that for any other variable X, $|X(t)| < \delta$. Comparing the solution of system (1) with the one of the linear system (21), as in Theorem 5, we obtain that

$$X(t) \leq ke^{-\min\{|u|,\mu\}t} \max\{E(0), I(0), A(0), H(0), R(0)\}. \tag{43}$$

Since $\| P(0) - P^* \| < \epsilon$, we have that

$$X(t) \leq k\epsilon e^{-\min\{|u|,\mu\}t} \leq k\epsilon, \tag{44}$$

and in particular

$$I(t) + A(t) \leq 2k\epsilon e^{-\min\{|u|,\mu\}t}. \tag{45}$$

Now, from the first equation of system (1)

$$-\beta(I(t) + A(t)) \leq S'(t) \leq \Lambda(I(t) + A(t)), \tag{46}$$

which implies that

$$|S'(t)| \leq \max\{\beta, \Lambda\} 2k\epsilon e^{-\min\{|u|,\mu\}t}. \tag{47}$$

Using the fundamental theorem of calculus

$$\begin{aligned} |S(t) - S(0)| &= \left| \int_0^t S'(x)dx \right| \leq \max\{\beta, \Lambda\} 2k\epsilon \int_0^t e^{-\min\{|u|,\mu\}x} dx = \\ &\max\{\beta, \Lambda\} k\epsilon \frac{1}{\min\{|u|, \mu\}} \left(1 - e^{-\min\{\mu\}t}\right) \leq 2k \frac{\max\{\beta, \Lambda\}}{\min\{|u|, \mu\}} \epsilon = L\epsilon. \end{aligned} \tag{48}$$

Taking $\epsilon < \frac{\delta}{L+1}$ and $\epsilon < \frac{\delta}{k}$, we deduce

$$|S(t) - S^*| \leq |S(t) - S(0)| + |S(0) - S^*| \leq (L+1)\epsilon < \delta, \tag{49}$$

and

$$|x(t)| < \delta, \tag{50}$$

which proves the stability. □

Theorem 7 proves that if $R_0 > 1$ all the equilibrium points with $S^* > 0$ are unstable, but the origin is a globally stable point. The COVID-19 disease has a high transmission (due to SARS-CoV-2 virus is very contagious) and S goes to zero quickly or well the infection remains active for a long time.

If $R_0 < 1$, the theorem states the stability of the equilibrium points with $S^* > 0$, but does not states the stability or the unstability of the origin. However, if (31) is satisfied, the origin is unstable. The infection disappears with time and the population tends to a stable value $N^* = S^*$.

2.4.4. Case $\Lambda = \mu = 0$

This is a particular case of $\Lambda = \mu$, so the total population obeys the following equation

$$dN/dt = -\delta H.$$

Total population N decreases if $H \geq 0$, this means that $N(t)$ has a limit $N^* \geq 0$. The difference with the general case $\Lambda = \mu$ is that in this case the critical points are $P^* = (S^*, 0, 0, 0, 0, R^*)^T$ at which the Jacobian matrix of the system (1) is

$$J = \begin{pmatrix} 0 & 0 & -\frac{\beta S^*}{S^*+R^*} & -\frac{\beta S^*}{S^*+R^*} & 0 & 0 \\ 0 & -(\sigma) & \frac{\beta S^*}{S^*+R^*} & \frac{\beta S^*}{S^*+R^*} & 0 & 0 \\ 0 & p\sigma & -(\gamma) & 0 & 0 & 0 \\ 0 & (1-p)\sigma & 0 & -(k_1) & 0 & 0 \\ 0 & 0 & \gamma & 0 & -(k_2+\delta) & 0 \\ 0 & 0 & 0 & k_1 & k_2 & 0 \end{pmatrix}.$$

This matrix has the eigenvalue 0 double. The eigenvectors associated with this eigenvalue are $(0,0,\ldots,1)^T$ and $(1,\ldots,0,0)^T$. This means that the component of the fundamental solution associated with the eigenvalue 0 only affects the first variable S and the last variable R. The behaviour of other variables will depend on the remaining four eigenvalues.

Another eigenvalue is $-(\delta+k_2)$, whose eigenvector is $(0,0,0,0,-\frac{k_2+\delta}{k_2},1)^T$. This means that the behaviour of the variables E, I and A depends on the three remaining eigenvalues, which are those of the main submatrix of dimension 3 obtained by eliminating the first and the last two rows and columns. This submatrix was already studied in Section 2.3, where we concluded that their three eigenvalues have negative real part if and only if

$$\hat{R}_0 \frac{S^*}{S^*+R^*} < 1, \tag{51}$$

with $\hat{R}_0$ the basic reproductive number with $\mu = 0$, that is

$$\hat{R}_0 = R_0(\mu=0) = \frac{\beta[\gamma(1-p)+k_1 p]}{k_1\gamma}, \tag{52}$$

which means that the equilibrium point is stable if

$$\frac{S^*+R^*}{S^*} > \hat{R}_0. \tag{53}$$

The global stability of the equilibrium points is studied in a similar way to the case $\Lambda = \mu$, so the following theorem can be stated.

Theorem 8. *All solution of the differential system (1) with $\Lambda = \mu = 0$, whose initial condition has all its components non negative, tends to an equilibrium point $(S^*,0,0,0,0,R^*)^T$ when t tends to infinity.*

In this case, if we apply the method employed in Section 2.3 we obtain precisely the condition (51).

Taking into account the local stability result, given an equilibrium point, the limit point S^* and R^* will be such that Eq. (53) is satisfied. In other words, the solution of system (1) will tend to an equilibrium point P^* for which S^* and R^* satisfy Eq. (53). As R_0 increases, S^* decreases and Eq. (53) is satisfied.

3. Results

3.1. Statistics

We use the simulation annealing algorithm for model fitting [25], in this process the sum of the squared errors between the original data and predicted values by model are minimized to obtain the best parameters for this fit. The quality of model fitting is verified by criteria for model assessment: r^2, *SSE*, *RMSE* [26] and relative error (RE) [3], given by

$$SSE = \sum_{j=1}^{n} \left(x_j - x_{jref}\right)^2, \tag{54}$$

$$1 - r^2 = \frac{\sum_{j=1}^{n}\left(x_j - x_{jref}\right)^2}{\sum_{j=1}^{n}\left(x_{jref}\right)^2 - \frac{1}{n}\sum_{j=1}^{n}\left(x_{jref}\right)^2}, \tag{55}$$

$$RMSE = \sqrt{\frac{\sum_{j=1}^{n}\left(x_j - x_{jref}\right)^2}{n}}, \tag{56}$$

$$RE = \sqrt{\frac{\left|\left|x - x_{ref}\right|\right|_2}{\left|\left|x_{ref}\right|\right|_2}}. \tag{57}$$

In Eq. (54)–(57), x_{ref} are data daily provided by the Ministry of Health, whereas x are those obtained from the model fitting, and n is the number of experimental data.

3.2. Simulation

In this section, we will validate the theoretical results obtained in Section 2 by considering several cases: the case where $\Lambda > \mu$ with $\Lambda = 0.015$ and $\mu = 0.01$, the case where $\Lambda < \mu$ with $\Lambda = 0.008$ and $\mu = 0.01$, the case where $\Lambda = \mu \neq 0$ with $\Lambda = 0.008$, and the case where $\Lambda = \mu = 0$. For each case we assume $N_{\max} = 100000$ and an initial population around 10000, ensuring that we are far from the carrying capacity $N_{\max}$. Additionally, we choose three values of β such that the corresponding values of R_0 (see Eq. 6 and 52) are smaller than, approximately equal to or grater than 1 (Table 2).

Table 2
Values of basic reproduction numbers R_0 for simulation of system (1).

β (days^{-1})	$\Lambda > \mu$ R_0	$\Lambda < \mu$ R_0	$\Lambda = \mu$ R_0	$\Lambda = \mu = 0$ R_0
0.05	0.3391	0.3391	0.3496	0.3975
0.20	1.3565	1.3565	1.3983	1.5910
1.00	6.7824	6.7824	6.9915	7.9500

Table 3
Value of each parameter for simulation and calculation of R_0.

Parameters	Values
Population	11380
$S(t=0) = S(0)$	8520
$E(t=0) = E(0)$	1000
$I(t=0) = I(0)$	100
$A(t=0) = A(0)$	80
$H(t=0) = H(0)$	200
$R(t=0) = R(0)$	0
p	0.5500
k_1^{-1} (days)	14
σ^{-1} (days)	5.1000
k_2^{-1} (days)	20
δ^{-1} (days)	15
γ^{-1} (days)	3

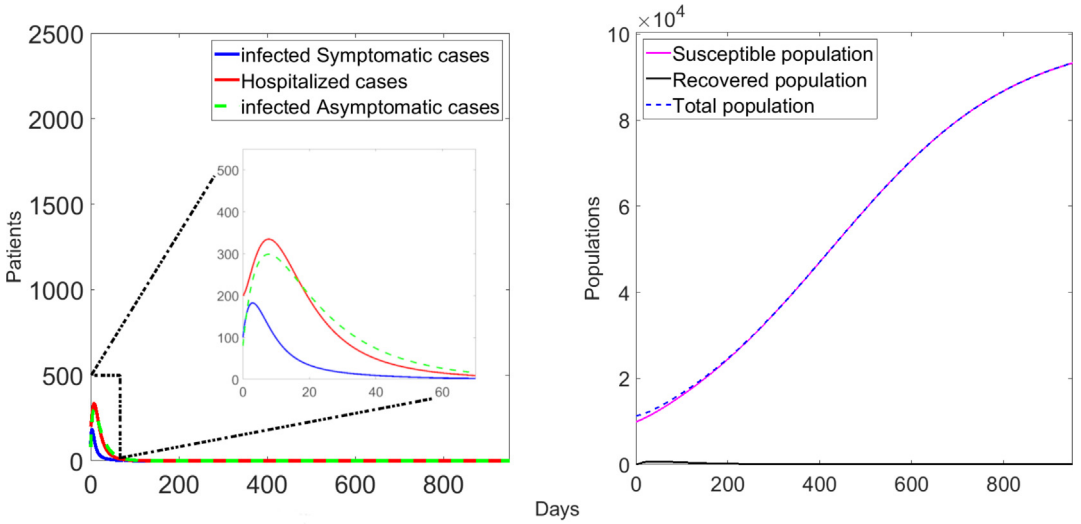

Fig. 2. Simulation of system (1) for $\Lambda = 0.015$, $\mu = 0.01$, $\beta = 0.05$ days^{-1} and $R_0 = 0.3391$. a) Infected symptomatic (blue line), hospitalized (red line) and infected asymptomatic (dashed green line) cases b) Susceptible (magenta line), recovered (black line) and total populations (dashed blue line).

The other parameters of the model and the initial conditions for those exposed, infected, infected asymptomatic, hospitalized and recovered cases are kept constant (Table 3).

Parameters values in Table 2 are taken arbitrarily, except σ^{-1} (in days) and k_1^{-1} (in days) that are those reported in [27]. Parameter values are kept constant to perform the calculation of R_0 and simulations of temporal behaviour of symptomatic (blue line), asymptomatic (dashed green line), hospitalized patients (red line), susceptible (magenta line) and recovered (black line) cases, as shown in Fig. 5 to Fig. 12. For numerical solution of the system (1), the ODE45 algorithm implemented in the Matrix Laboratory (MATLAB) is used [28].

3.2.1. Case $\Lambda > \mu$

Figures 2a, 3a and 4a show the temporal behaviour of infected symptomatic (blue line), hospitalized (red line) and infected asymptomatic (dashed green line) cases while in Figs. 2b, 3b and 4b the susceptible (magenta line), recovered (black line), and the total populations (dashed blue line) are shown.

The simulations reveal that the total population and the number of susceptible people grow with time, and the infected, asymptomatic and hospitalized cases tend to zero when $R_0 < 1$, in agreement with Theorems 3, 4 and 5, respectively. When $R_0 > 1$, the susceptible tend to the carrying capacity and the infected, asymptomatic and hospitalized grow with time. The

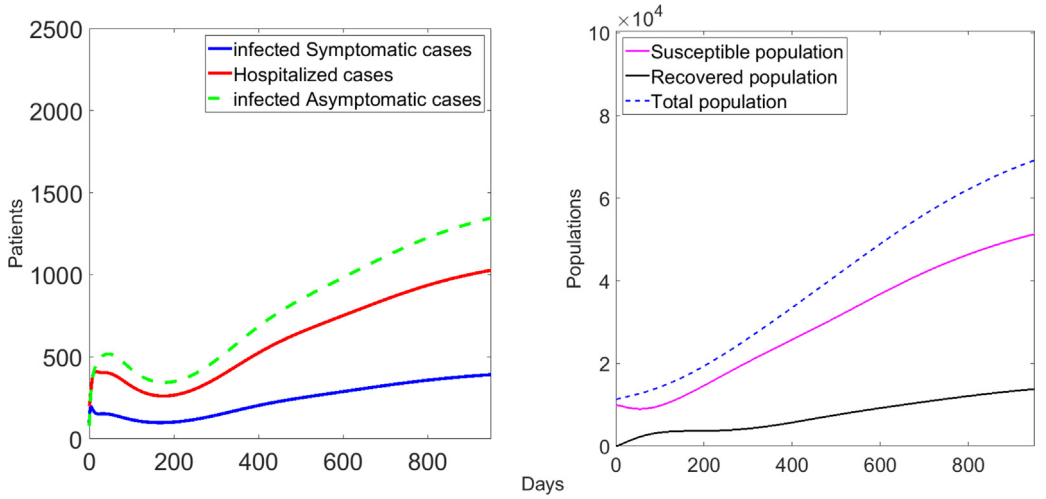

Fig. 3. Simulation of system (1) for $\Lambda = 0.015$, $\mu = 0.01$, $\beta = 0.2$ days^{-1} and $R_0 = 1.3565$. a) Infected symptomatic (blue line), hospitalized (red line) and infected asymptomatic (dashed green line) cases b) Susceptible (magenta line), recovered (black line) and total populations (dashed blue line).

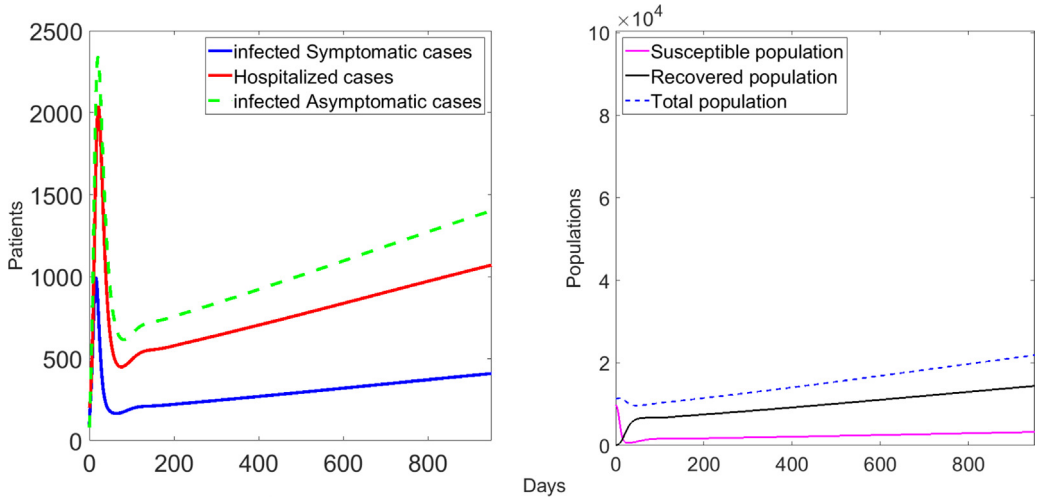

Fig. 4. Simulation of system (1) for $\Lambda = 0.015$, $\mu = 0.01$, $\beta = 1$ days^{-1} and $R_0 = 6.7824$. a) Infected symptomatic (blue line), hospitalized (red line) and infected asymptomatic (dashed green line) cases b) Susceptible (magenta line), recovered (black line) and total populations (dashed blue line).

number of infected people increases and the growth velocity of susceptible people decreases faster as R_0 increases. The number of hospitalized cases depends on the values of γ, β and R_0, showing different scenarios. First, hospitalized cases depend on the symptomatic and asymptomatic cases, as show in Figs. 2a, 3a and 4a. Second, the number of hospitalized cases is lower than that the asymptomatic cases when $R_0 \geq 1$ (Figs. 3a and 4a).

3.2.2. *Case* $\Lambda < \mu$

Figures 5a, 6a and 7a show the temporal behaviour of infected symptomatic (blue line), hospitalized (red line) and infected asymptomatic (dashed green line) cases while in Figs. 5b, 6b and 7b the susceptible (magenta line), recovered (black line), and the total populations (dashed blue line) are shown.

The simulation results reveal that the total population tends to zero in all the cases, in agreement with Theorem 6. Note that population decreases quickly initially, but after some time it decreases exponentially as $e^{-\mu t}$ and since μ is small, the decreasing is very slow. It can be verified that with a larger value of μ the population tends to zero much faster. For the shake of brevity we have not included this simulation in the paper and we have included the most realistic cases. The number of infected people increases and the value of susceptible people decreases faster as R_0 increases. The number of hospitalized cases depends on the values of γ, β and R_0, and two possible scenarios appear. First, hospitalized cases depend on infected symptomatic and asymptomatic cases with prevalence of asymptomatic patients (Figs. 5a, 6a and 7a). Second, the number of hospitalized patients is always less than the asymptomatic when $R_0 \geq 1$ (Figs. 6a and 7a).

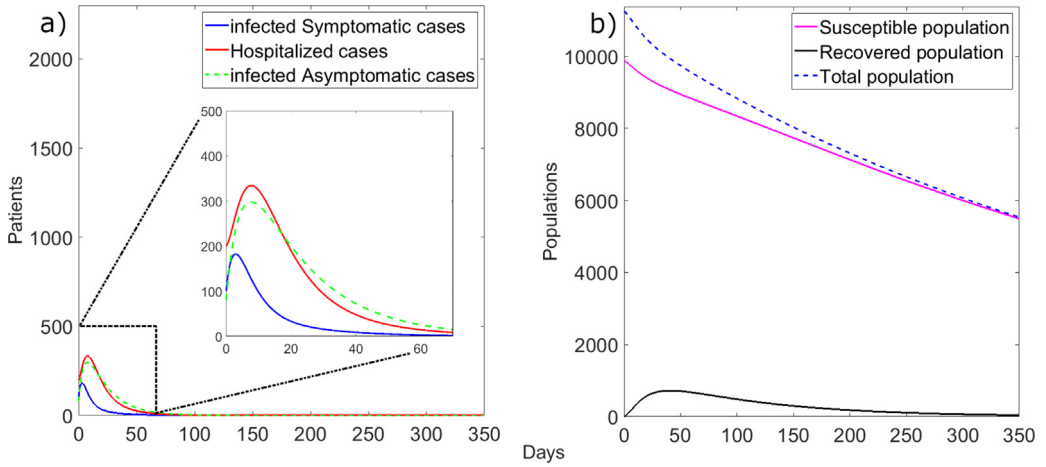

Fig. 5. Simulation of system (1) for $\Lambda = 0.008$, $\mu = 0.01$, $\beta = 0.05$ days^{-1} and $R_0 = 0.3391$. a) Infected symptomatic (blue line), hospitalized (red line) and infected asymptomatic (dashed green line) cases b) Susceptible (magenta line), recovered (black line) and total populations (dashed blue line).

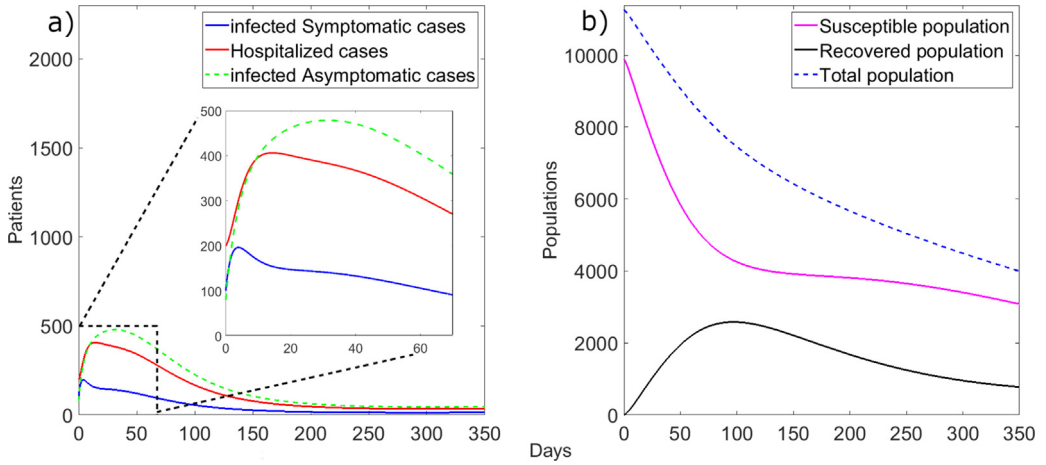

Fig. 6. Simulation of system (1) for $\Lambda = 0.008$, $\mu = 0.01$, $\beta = 0.2$ days^{-1} and $R_0 = 1.3565$. a) Infected symptomatic (blue line), hospitalized (red line) and infected asymptomatic (dashed green line) cases b) Susceptible (magenta line), recovered (black line) and total populations (dashed blue line).

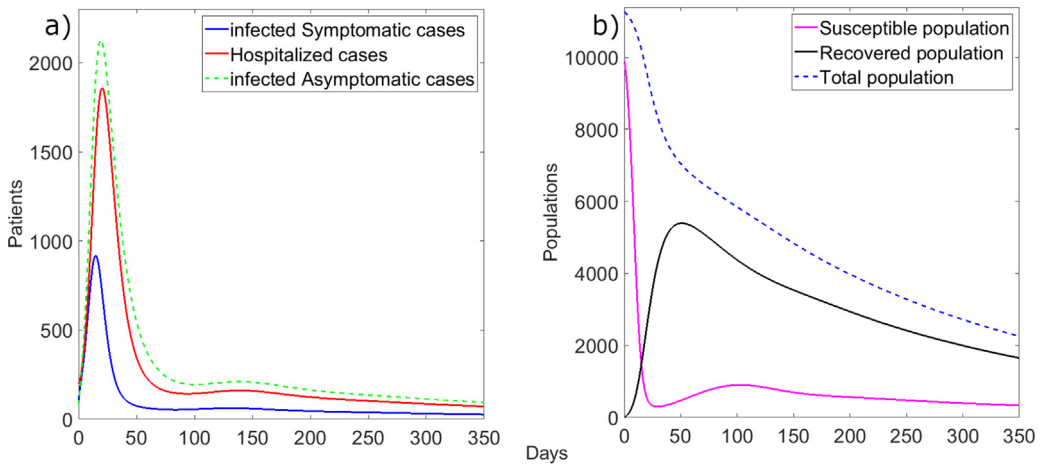

Fig. 7. Simulation of system (1) for $\Lambda = 0.008$, $\mu = 0.01$, $\beta = 1$ days^{-1} and $R_0 = 6.7824$. a) Infected symptomatic (blue line), hospitalized (red line) and infected asymptomatic (dashed green line) cases b) Susceptible (magenta line), recovered (black line) and total populations (dashed blue line).

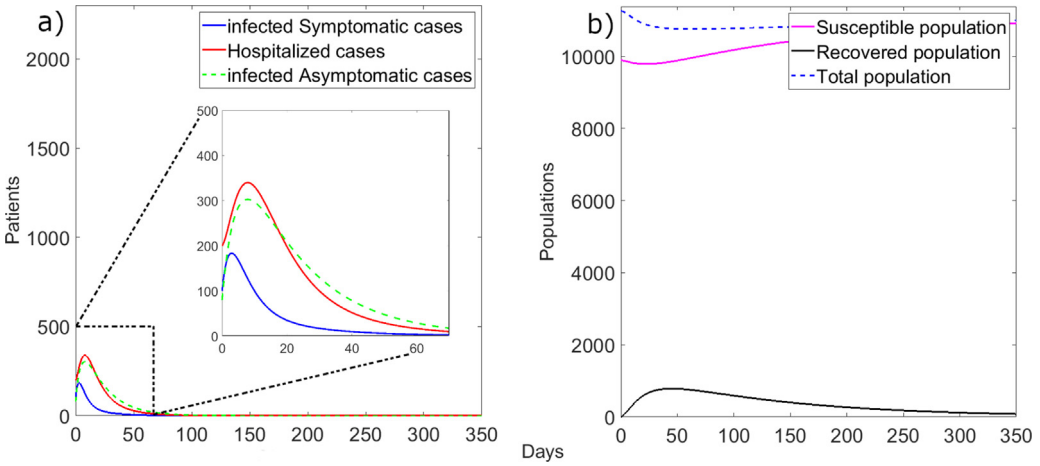

Fig. 8. Simulation of system (1) for $\Lambda = 0.008$, $\mu = 0.008$, $\beta = 0.05$ days^{-1} and $R_0 = 0.3496$. a) Infected symptomatic (blue line), hospitalized (red line) and infected asymptomatic (dashed green line) cases b) Susceptible (magenta line), recovered (black line) and total populations (dashed blue line).

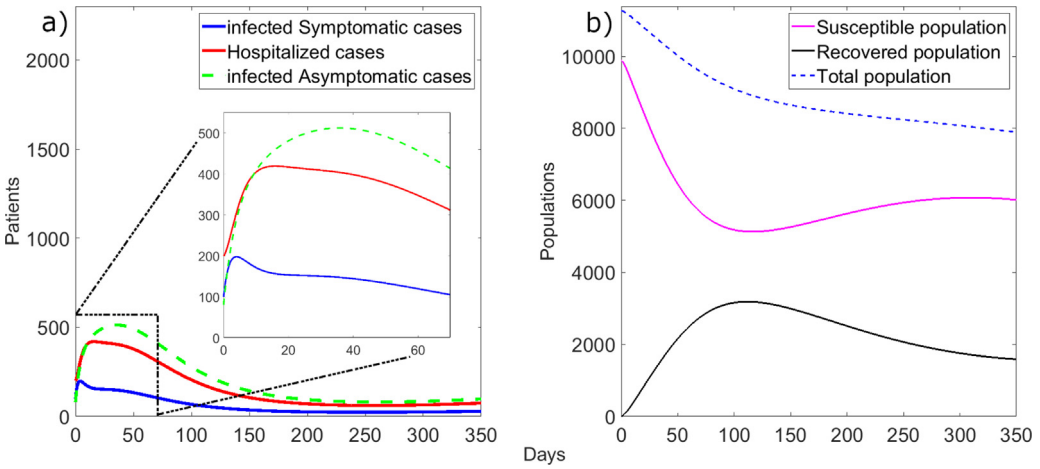

Fig. 9. Simulation of system (1) for $\Lambda = 0.008$, $\mu = 0.008$, $\beta = 0.2$ days^{-1} and $R_0 = 1.3983$. a) Infected symptomatic (blue line), hospitalized (red line) and infected asymptomatic (dashed green line) cases b) Susceptible (magenta line), recovered (black line) and total populations (dashed blue line).

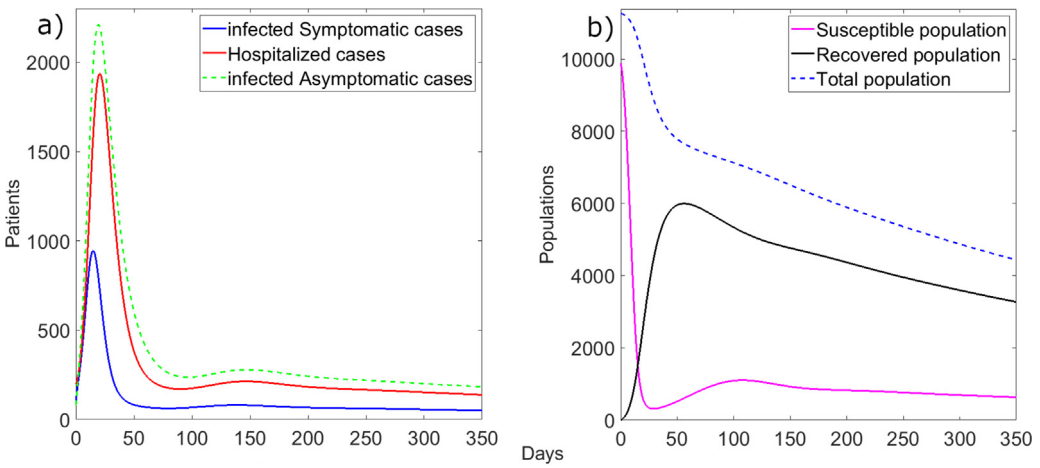

Fig. 10. Simulation of system (1) for $\Lambda = 0.008$, $\mu = 0.008$, $\beta = 1$ days^{-1} and $R_0 = 6.9915$. a) Infected symptomatic (blue line), hospitalized (red line) and infected asymptomatic (dashed green line) cases b) Susceptible (magenta line), recovered (black line) and total populations (dashed blue line).

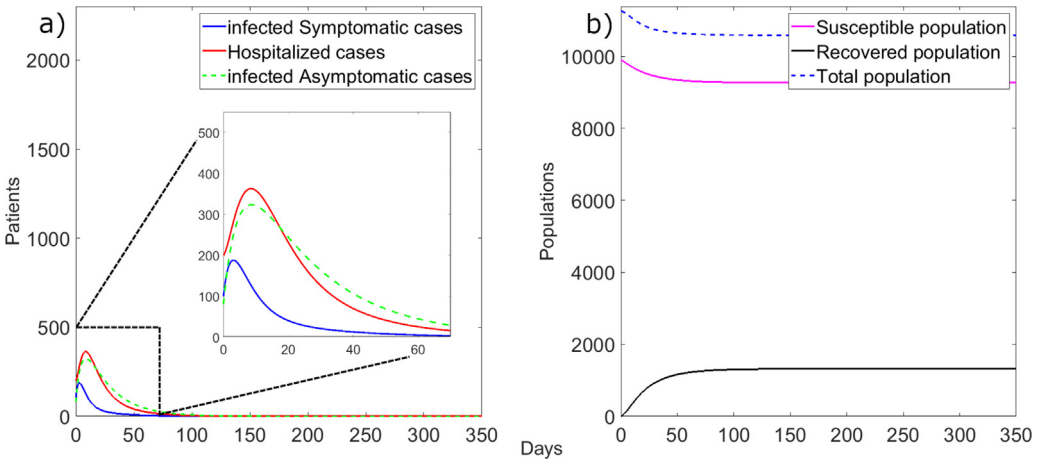

Fig. 11. Simulation of system (1) for $\Lambda = 0$, $\mu = 0$, $\beta = 0.05$ days^{-1} and $R_0 = 0.3975$. a) Infected symptomatic (blue line), hospitalized (red line) and infected asymptomatic (dashed green line) cases b) Susceptible (magenta line), recovered (black line) and total populations (dashed blue line).

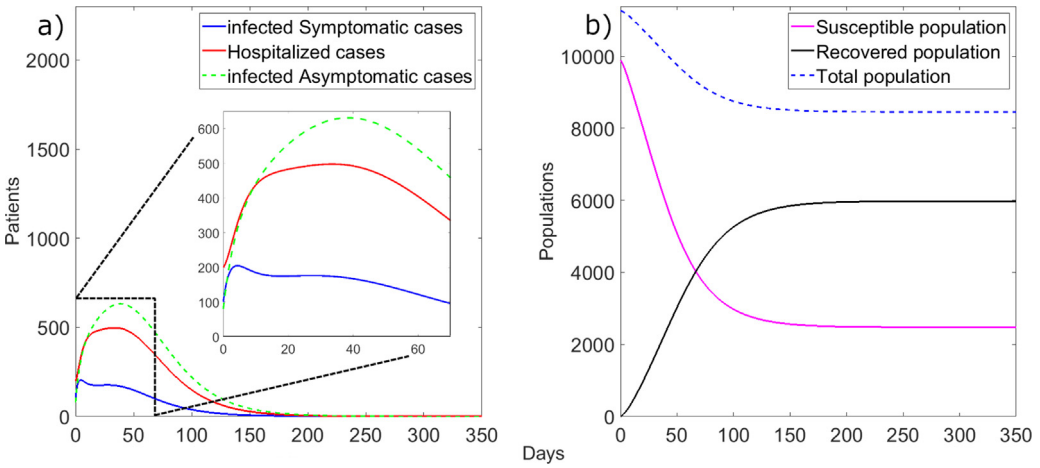

Fig. 12. Simulation of system (1) for $\Lambda = 0$, $\mu = 0$, $\beta = 0.2$ days^{-1} and $R_0 = 1.5910$. a) Infected symptomatic (blue line), hospitalized (red line) and infected asymptomatic (dashed green line) cases b) Susceptible (magenta line), recovered (black line) and total populations (dashed blue line).

3.2.3. *Case* $\Lambda = \mu$

Figures 8a, 9a, 10a show the temporal behaviour of infected symptomatic (blue line), hospitalized (red line) and infected asymptomatic (dashed green line) cases while in Figs. 8b, 9b, 10b the susceptible (magenta line), recovered (black line) and the total populations (dashed blue line) are shown.

The simulation results reveal that the solution of system (1) tends to an equilibrium point $(S^*, 0, 0, 0, 0, 0)$, in all the cases, in agreement with Theorem 7. The value of S^* depends on R_0 and decreases as R_0 increases. For $R_0 > 1$, the infected, asymptomatic and hospitalized tend to zero, very slowly, and S^* is zero, in agreement with Theorem 7. The total population N tends to zero faster as R_0 increases. The number of hospitalized cases depends on the values of γ, β y R_0, showing different possible scenarios. First, hospitalized cases depend on the symptomatic and asymptomatic infected, as shown in Figs. 8a, 9a, 10a. Second, the number of hospitalized patients is always lower than the asymptomatic when $R_0 \geq 1$, as can be seen in the Figs. 9a, 10a.

3.2.4. *Case* $\Lambda = \mu = 0$

Figures 11a, 12a, 13a show the temporal behaviour of infected symptomatic (blue line), hospitalized (red line) and infected asymptomatic infected (dashed green line) cases while in Figs. 11b, 12b, 13b the susceptible (magenta line), recovered (black line) and the total populations (dashed blue line) are shown.

The simulation results reveal that the solution tends in all the cases to an equilibrium point $(S^*, 0, 0, 0, 0, R^*)$, in agreement with Theorem 8. For $R_0 < 1$, the value S^* is not far from the initial value S_0 and most of the people do not suffer the infection. The total population decreases due to the infection, but not much. The effect of the disease is moderated. For $R_0 \approx 1$, the values of S^* and R^* are smaller and larger respectively than the ones for $R_0 < 1$. The population decreases a little more and the effect of the disease is more important than in the previous case. For $R_0 > 1$, S^* is close to zero, which means that almost the whole population gets infected (the recovered people is practically equal to the total population). The

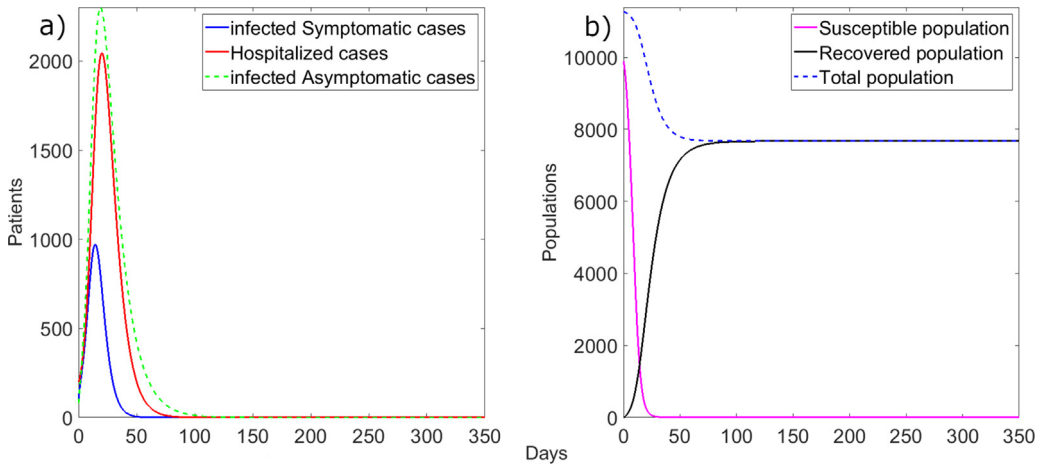

Fig. 13. Simulation of system (1) for $\Lambda = 0$, $\mu = 0$, $\beta = 1$ days^{-1} and $R_0 = 7.9500$. a) Infected symptomatic (blue line), hospitalized (red line) and infected asymptomatic (dashed green line) cases. b) Susceptible (magenta line), recovered (black line) and total populations (dashed blue line).

Table 4
Parameters obtained from model fitting COVID-19 data of Republic of Cuba.

Parameters	Values
Population	11201549
Λ	$2.68\text{x}10^{-5}$
μ	$2.67\text{x}10^{-5}$
β	0.2027
p	0.5995
k_1^{-1} (days)	14.0000
σ^{-1} (days)	5.1000
k_2^{-1} (days)	10.8342
δ^{-1} (days)	19.6516
γ^{-1} (days)	1.4384
R_0	1.3107

population is clearly reduced and the effect of the epidemic is remarkable. The number of hospitalized cases depends on the values of γ, β y R_0. These show different possible scenarios. First, hospitalized cases depend on the symptomatic and asymptomatic infected as shown in Figs. 11a, 12a, 13a. Second, the number of hospitalized patients is always lower than the asymptomatic when $R_0 \geq 1$, as can be seen in the Figs. 12a and 13a.

4. Model fitting

To fit system (1), we used official data of accumulated, infected, hospitalized and eliminated cases of COVID-19 in Cuba provided by the Ministry of Public Health (MINSAP) that displayed on the web platform (https://covid19cubadata.github.io). We chose data reported for 429 days of pandemic from March 12, 2020 to May 15, 2021 for Cuba. The total population ($N(0)$), the birth rate (Λ) and death rate (μ) are calculated from the data reported in the MINSAP statistical yearbook [29]. Values of latent time, σ^{-1} (in days), and the average recovery time of asymptomatic patients (k_1^{-1}, in days) are taken from Lauer et al. [27]. Initial values of infected ($I(0)$) and hospitalized ($H(0)$) cases are taken from official data. The initial susceptible ($S(0)$) and recovered ($R(0)$) are assumed equal to 99% of total population and zero, respectively. Finally, the values of initial asymptomatic patient ($A(0)$), initial exposed patient ($E(0)$), Λ, β, p, δ^{-1}, γ^{-1} and k_2^{-1} are estimated from model.

Fitting the model to the data by a least squares approach, we obtain the parameters shown in Table 4. Figure 14 shows experimental data (for symptomatic and hospitalized cases), model fitting (for symptomatic and hospitalized cases) and simulation of infected asymptomatic cases. We can see from this figure that the model fits data of number of infected symptomatic cases but not for hospitalized cases. It is important to point out that all the infected (symptomatic and asymptomatic) cases and suspected individuals of COVID-19 are hospitalized in the Republic of Cuba. Nevertheless, in the model the hospitalized are a fraction of these infected cases.

The value of $R_0 = 1.3107$ obtained from model fitting is close to that reported from experimental data corresponding to March 13, 2020 ($R_0 = 1.3457$). Both R_0 values corroborate our simulations corresponding to the case $R_0 \approx 1$ and $\Lambda = \mu$. Values of criteria for model assessment proposed in Section 3.1 are shown in Table 5.

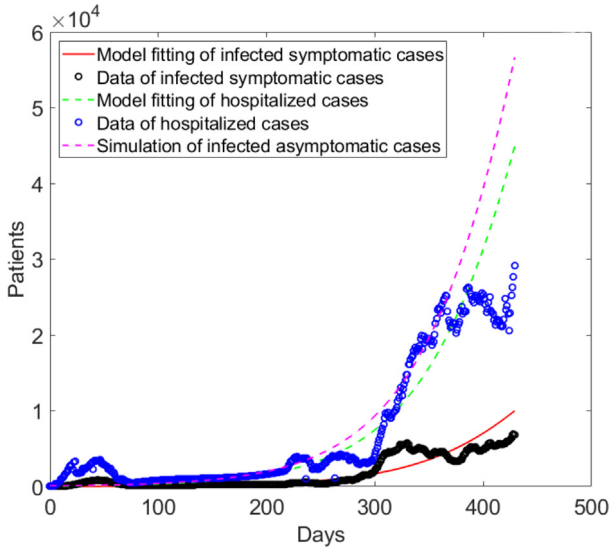

Fig. 14. Fit of system (1) from March 12, 2020 to May 15, 2021.

Table 5
Parameter values of quality of the model fitting.

Parameters	Symptomatic cases	Hospitalized cases
r^{2a}	0.8533	0.8917
SSE^b	1.1751×10^3	4.4926×10^3
$RMSE^c$	1.600×10^3	4.4348×10^3
RE^d	0.3825	0.3287

[a]Goodness of fit, [b]Sum of squares error, [c]Root mean square error, [d]Relative error

5. Discussion

The modified SEIR model fits well to the reported COVID-19 data with r^2 in the range $0.85 - 0.89$. It is plausible that the supplied data, has many fluctuations and likely subject to a large uncertainty. It may be mentioned: 1) fluctuacting behaviours in the number of active and hospitalized cases due to unwanted epidemiological events in the Republic of Cuba. These unwanted epidemiological events are due to native transmission and transmission by travellers originating in other countries with high COVID-19 transmission and new strains of SARS-CoV-2. 2) Introduction of new strains of SARS-CoV-2, as South Africa (variant B.1.551), United Kingdom (variant B.1.1.7), California (variant B.1.429), Brazil (variants B.1.1.28.1 and B.1.2.28.2), and India (variant B.1.617 or delta strain). These strains have higher transmission rates than original Wuhan strain (variant D614G), which prevails in the Republic of Cuba from March 2020 up to April 2021. 3) Seven new protocols for confrontation to COVID-19 that have been introduced according to epidemiological situation. 4) Clinical trials (Phases I-III) of Abdala and Soberana-02 vaccine candidates. These reasons explain why model fitting system (1) of experimental data is not totally good in the study period selected, one of limitations of this study. Another limitation of this study is that β and R_0 are considered constants in our model; nevertheless, epidemiological studies evidence that these two parameters change over time [21,22,30–32].

These two above-mentioned limitations may be solved if this study period is analyzed by section, taking into account the protocol, transmission rate of SARS-CoV-2 strain type, government measures, perception risk of individuals and social responsibility of individuals. For this, a further study is being carried out.

Despite these two limitations, β, p and R_0 values obtained from model fitting to experimental data (Table 4) agree with epidemiological data reported every week to MINSAP, from November 2020 up to the end May 2021. $\beta = 0.2027$ days^{-1} agrees with its β values ($0.2 \leq \beta \leq 0.4$) reported in [20,33]. $R_0 = 1.3107$ belongs to interval $[0.068, 2.85]$, agrees with reported daily by MINSAP.

Simulations and model fitting to experimental data corroborate that the propagation of the COVID-19 disease depends on R_0 (Eq. (6) and (52)), which is directly proportional to β and p parameters, in agreement with the definition itself of R_0 [30–32]. If the time behaviour of β (named $\beta(t)$) reported in [20] is introduced in Eq. (6) and (52), we would corroborate that R_0 depends also on t, in agreement with [21,22,30–32].

On the other hand, R_0 is directly related to p and its value may contribute to speed up COVID-19 propagation (see Eqs. (6) and (52)). The value obtained for $p = .5995$ is consistent with the rapid spread of COVID-19 and prevalence of symptomatic cases in the period March 2020 - May 2021. This does not mean that asymptomatic cases become infected later and/or they are capable of infecting other susceptible individuals. This depends on the type of dominant and circulat-

ing SARS-CoV-2 strain, strenght of immune system (immunodeficient and immunocompetent patients), and environmental conditions. It should be noted that these asymptomatic patients are not hospitalized because they have no symptoms or are mild. Furthermore, none of them die. Nevertheless, some unvaccinated cases with comorbidities die when they are infected with the Delta variant. These deceased cases are reported from June 2021.

From epidemiological point of view, $p = .5995$ means that more than half of the infected cases are detected, indicating that the government policy in the COVID-19 confrontation is correct. Furthermore, this p value agrees with the number of asymptomatic cases reported in the Republic of Cuba (55.0%) in this observation period, in agreement with [34].

The values of k_2^{-1}, δ^{-1} and γ^{-1} obtained from model fitting of experimental data (Table 4) allow to consider that μ can be neglected respect to k_1, γ and σ in Eqs. (6) and (52). As μ is very small, R_0 does not change significantly with σ. This confirms that R_0 does not depend on incubation time of any SARS-CoV-2 strain in the host but infected individual that has associated an average number of infected contacts (definition of R_0) [30–32]. Furthermore, the definition itself of R_0 justifies that it does not depend on δ and k_2 either. This is also expected because in our model it is assumed that a hospitalized person does not contribute to generate new infected. Nevertheless, δ value is very important because it directly affects the number of deaths due to the infection. In these situations, R_0 is dominated by β and p, as expected. Additionally, results of Table 4 and μ very small allow to obtain an expression for R_0 when $p = 0$ proportional to ${}^{\beta}/_{k_1}$, this suggest that when p is small the progression of the disease depends on the recovery time average of asymptomatic patients k_1^{-1}. On the other hand, if $p = 1$ we can obtain an expression for R_0 proportional to ${}^{\beta}/_{\gamma}$, this suggest that for p large (close to 1) the progression of the disease will depend on the time between symptoms onset to hospiltalization γ^{-1}. Taking into account that ${}^{1}/_{k_1}$ is larger than $1/\gamma$, we conclude that p large will give smaller values of R_0. Consequently, policies tending to get p as large as possible, and making γ as large as possible (k_1 depends on the disease and can not be modified) will reduce the value of R_0.

From temporal behaviour of symptomatic, asymptomatic and hospitalized cases, it can be observed that these take their maximum value depending on the β, γ and R_0 values, as shown in the Figs. 5 to 13. For case $\Lambda < \mu$, the number of Infected cases (I) always reaches its minimum value at zero and its quick growth depends strongly on R_0. Nevertheless, the number of infected cases for $\Lambda = \mu$ and $\Lambda = \mu = 0$ always reaches a minimum value at zero and this depends on the R_0 value, being remarkable for $\Lambda = \mu$.

The simulation and fit of proposed model, resulted in that if the time between symptom onset to hospitalization (γ^{-1}) increases, the average of hospitalization time (k_2^{-1}) and average of time that an hospitalized patient died (δ) also increases. This fact, suggests that the earlier the treatment protocol is started, the less time the patient is hospitalized, as suggested in [35]. Nevertheless, if we analyse the pandemic in two periods of time the average of time that an hospitalized patient died (δ) should increase due to the development of new treatment protocols [36] but did not vary much. This may be justified by the presence of new SARS-CoV-2 strains with higher virulence, pathogenicity, invasiveness, and diffusibility, as delta variant.

The number of symptomatic cases higher than that hospitalized cases is not observed in Republic of Cuba. Simulations reveal this unfavourable scenery when the time between symptom onset to hospitalization (γ^{-1}) increases. This suggest, that the active search of infected can help to control the pandemic.

6. Conclusion

We have proposed a modified SEIR mathematical model that explicitly includes asymptomatic and hospitalized cases, to help the epidemiological study of infectious diseases, as evidenced for COVID-19. We have also included the effect of demography in the model, considering that the population grows proportionally to the total population, which leads to solutions with behavior that differs from those obtained in models where the ratio is considered constant. We have studied the stability of the model and we have verified these stability results with some numerical simulations. We computed and verified the basic reproduction number corresponding to the model and showed that this number determines the qualitative evolution of the disease. This model was fitted with experimental data from Republic of Cuba and we have shown that it model reproduces the evolution of the experimental data. This suggest that the model can be a useful tool. Nevertheless, this model is adequate only for one peak, and this is the reason why research is continuing to obtain an algorithm to improve these results.

Data availability

Data will be made available on request.

Acknowledgments

The authors thank the editor and anonymous reviewers for their valuable suggestions that greatly improved this manuscript. This research is supported by the doctoral scholarship from the Universidad de Zaragoza-Santander Universidades program and the projects PID2019-109045GB-C31 of Ministery of Science and Innovation of Spain, Furthermore, We thank Professor PhD. Jesús Carnicer for his help in the proof of Lemma 1.

Appendix A

Figure A.1

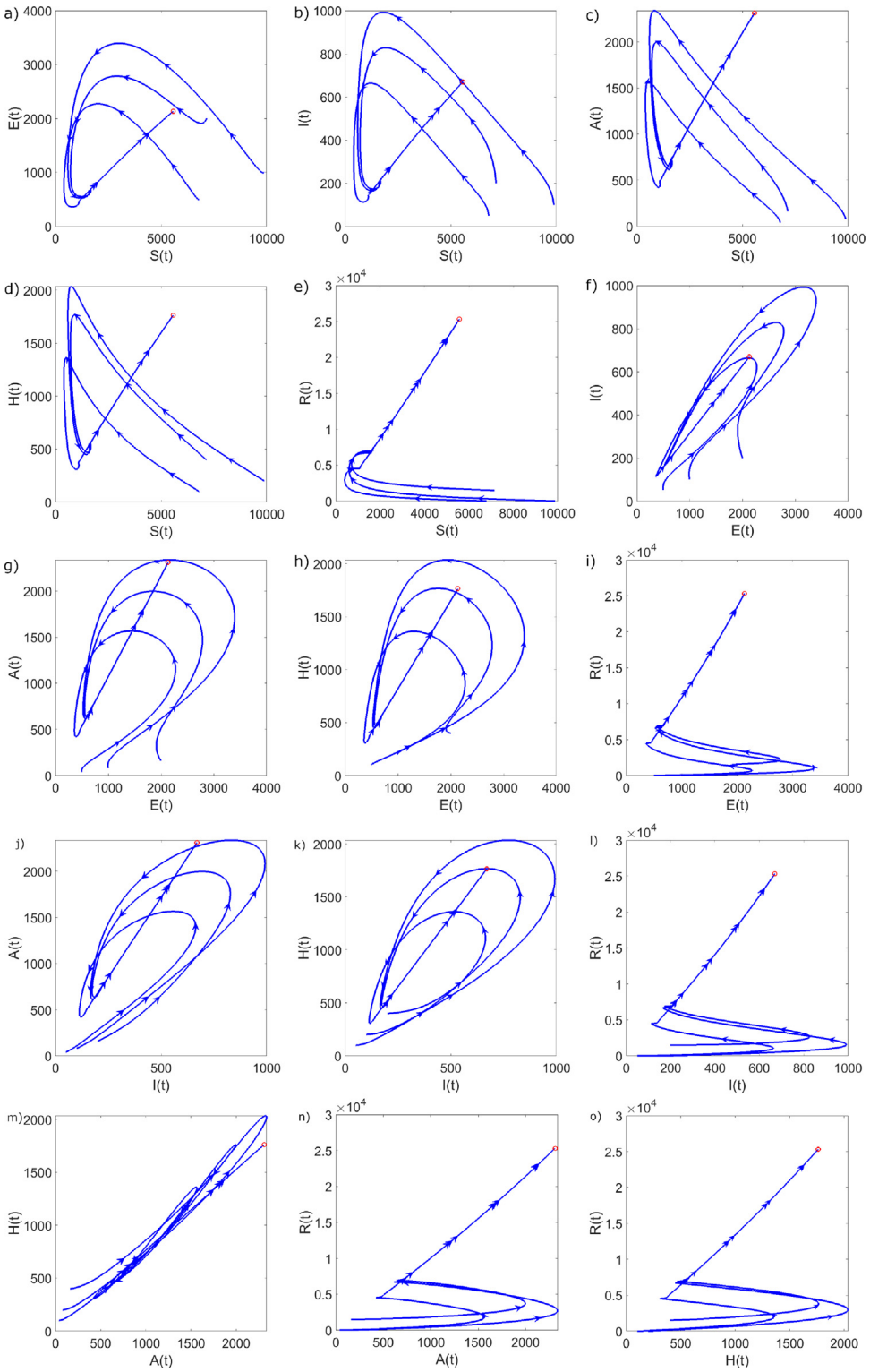

Fig. A.1. Phase portrait of system (1) for different initial conditions (blue line) and equilibrium point (red).

References

[1] W.O. Kermack, A.G. McKendrick, A contribution to the mathematical theory of epidemics, Proc. R. Soc. London Ser.A 115 (772) (1927) 700–721, doi:10.1098/rspa.1927.0118.
[2] M. Martcheva, An Introduction to Mathematical Epidemiology, Vol. 61, Springer, 2015, doi:10.1007/978-1-4899-7612-3.
[3] L. Peng, W. Yang, D. Zhang, C. Zhuge, L. Hong, Epidemic analysis of COVID-19 in China by dynamical modeling, arXiv preprint arXiv:2002.06563(2020).
[4] A.G. Neves, G. Guerrero, Predicting the evolution of the COVID-19 epidemic with the A-SIR model: Lombardy, Italy and Sao Paulo State, Brazil, Physica D 413 (2020) 132693, doi:10.1016/j.physd.2020.132693.
[5] R. Li, S. Pei, B. Chen, Y. Song, T. Zhang, W. Yang, J. Shaman, Substantial undocumented infection facilitates the rapid dissemination of novel coronavirus (SARS-CoV-2), Science 368 (6490) (2020) 489–493, doi:10.1126/science.abb3221. Publisher: American Association for the Advancement of Science
[6] W. McKibbin, R. Fernando, The global macroeconomic impacts of COVID-19: seven scenarios, Asian Econ. Pap. 20 (2) (2021) 1–30, doi:10.1162/asep_a_00796.
[7] E. Estrada, COVID-19 and SARS-CoV-2. modeling the present, looking at the future, Phys. Rep. 869 (2020) 1–51, doi:10.1016/j.physrep.2020.07.005. COVID-19 and SARS-CoV-2. Modeling the present, looking at the future
[8] F. Saldaña, J.X. Velasco-Hernández, Modeling the COVID-19 pandemic: a primer and overview of mathematical epidemiology, SeMA J. (2021) 1–27, doi:10.1007/s40324-021-00260-3.
[9] L. Brugnano, F. Iavernaro, P. Zanzottera, A multiregional extension of the SIR model, with application to the COVID-19 spread in Italy, Math. Methods Appl. Sci. 44 (6) (2021) 4414–4427, doi:10.1002/mma.7039.
[10] F. Ndaïrou, I. Area, J.J. Nieto, D.F. Torres, Mathematical modeling of COVID-19 transmission dynamics with a case study of Wuhan, Chaos Solitons Fractals 135 (2020) 109846, doi:10.1016/j.chaos.2020.109846.
[11] Q. Lin, S. Zhao, D. Gao, Y. Lou, S. Yang, S.S. Musa, M.H. Wang, Y. Cai, W. Wang, L. Yang, A conceptual model for the coronavirus disease 2019 (COVID-19) outbreak in wuhan, china with individual reaction and governmental action, Int. J. Infect. Dis. 93 (2020) 211–216, doi:10.1016/j.ijid.2020.02.058. Publisher: Elsevier
[12] J. Mena-Lorcat, H.W. Hethcote, Dynamic models of infectious diseases as regulators of population sizes, J. Math. Biol. 30 (7) (1992) 693–716, doi:10.1007/BF00173264.
[13] S. Ottaviano, M. Sensi, S. Sottile, Global stability of SAIRS epidemic models, Nonlinear Anal. Real World Appl. 65 (2022) 103501, doi:10.1016/j.nonrwa.2021.103501.
[14] Z. Hu, Z. Teng, H. Jiang, Stability analysis in a class of discrete SIRS epidemic models, Nonlinear Anal. Real World Appl. 13 (5) (2012) 2017–2033, doi:10.1016/j.nonrwa.2011.12.024.
[15] S. Saha, G. Samanta, J.J. Nieto, Epidemic model of COVID-19 outbreak by inducing behavioural response in population, Nonlinear Dyn. 102 (1) (2020) 455–487.
[16] C. Yang, J. Wang, A mathematical model for the novel coronavirus epidemic in Wuhan, China, Math. Biosci. Eng. 17 (3) (2020) 2708–2724, doi:10.3934/mbe.2020148.
[17] K. Shah, R.U. Din, W. Deebani, P. Kumam, Z. Shah, On nonlinear classical and fractional order dynamical system addressing COVID-19, Results Phys. 24 (2021) 104069, doi:10.1016/j.rinp.2021.104069.
[18] M. Shoaib, M.A.Z. Raja, M.T. Sabir, A.H. Bukhari, H. Alrabaiah, Z. Shah, P. Kumam, S. Islam, A stochastic numerical analysis based on hybrid NAR-RBFS networks nonlinear SITR model for novel COVID-19 dynamics, Comput. Methods Programs Biomed. 202 (2021) 105973, doi:10.1016/j.cmpb.2021.105973.
[19] R.M. Anderson, R.M. May, Population biology of infectious diseases: Part I, Nature 280 (5721) (1979) 361–367, doi:10.1038/280361a0.
[20] E.E. Ramirez-Torres, A.S. Castaneda, Y. Rodríguez-Aldana, S.S. Domínguez, L.V. García, A. Palú-Orozco, E.R. Oliveros-Domínguez, L. Zamora-Matamoros, R. Labrada-Claro, M. Cobas-Batista, Mathematical modeling and forecasting of COVID-19: experience in Santiago de Cuba province, Revista Mexicana de Física 67 (1 Jan-Feb) (2021) 123–136, doi:10.31349/RevMexFis.67.123.
[21] O. Diekmann, J.A.P. Heesterbeek, M.G. Roberts, The construction of next-generation matrices for compartmental epidemic models, J. R. Soc. Interface 7 (47) (2010) 873–885, doi:10.1098/rsif.2009.0386. Publisher: The Royal Society
[22] A. Perasso, An introduction to the basic reproduction number in mathematical epidemiology, ESAIM Proc. Surv. 62 (2018) 123–138, doi:10.1051/proc/201862123. Publisher: EDP Sciences
[23] V. Lakshmikantham, S. Leela, Differential and Integral Inequalities: Theory and Applications: Volume I: Ordinary Differential Equations, Academic press, 1969.
[24] A. McNabb, Comparison theorems for differential equations, J. Math. Anal. Appl. 119 (1) (1986) 417–428, doi:10.1016/0022-247X(86)90163-0.
[25] L. Ingber, Simulated annealing: practice versus theory, Math. Comput. Model. 18 (11) (1993) 29–57. Publisher: Elsevier
[26] M.M. González, J.A.G. Joa, L.E.B. Cabrales, A.E.B. Pupo, B. Schneider, S. Kondakci, H.M.C. Ciria, J.B. Reyes, M.V. Jarque, M.A.O. Mateus, Is cancer a pure growth curve or does it follow a kinetics of dynamical structural transformation? BMC Cancer 17 (1) (2017) 1–14, doi:10.1186/s12885-017-3159-y. Publisher: BioMed Central
[27] S.A. Lauer, K.H. Grantz, Q. Bi, F.K. Jones, Q. Zheng, H.R. Meredith, A.S. Azman, N.G. Reich, J. Lessler, The incubation period of coronavirus disease 2019 (COVID-19) from publicly reported confirmed cases: estimation and application, Ann. Intern. Med. 172 (9) (2020) 577–582, doi:10.7326/M20-0504. Publisher: American College of Physicians
[28] R. VRÁBEL', V. LIŠKA, J. Vaclav, Remark on sensitivity of simulated solutions of the nonlinear dynamical system to the used numerical method, Int. J. Math. Anal. 9 (43) (2015) 2749–2754, doi:10.12988/ijma.2015.59236.
[29] MINSAP, ANUARIO ESTADÁSTICO DE SALUD, 2019, http://files.sld.cu/bvscuba/files/2020/05/Anuario-Electrónico-Espa˜nol-2019-ed-2020.pdf.
[30] C. Fraser, C.A. Donnelly, S. Cauchemez, W.P. Hanage, M.D. Van Kerkhove, T.D. Hollingsworth, J. Griffin, R.F. Baggaley, H.E. Jenkins, E.J. Lyons, T. Jombart, W.R. Hinsley, N.C. Grassly, F. Balloux, A.C. Ghani, N.M. Ferguson, A. Rambaut, O.G. Pybus, H. Lopez-Gatell, C.M. Alpuche-Aranda, I.B. Chapela, E.P. Zavala, D.M.E. Guevara, F. Checchi, E. Garcia, S. Hugonnet, C. Roth, T.W.R.P.A. Collaboration, Pandemic potential of a strain of influenza a (H1N1): early findings, Science 324 (5934) (2009) 1557–1561, doi:10.1126/science.1176062.
[31] K.T.L. Sy, L.F. White, B.E. Nichols, Population density and basic reproductive number of COVID-19 across United States counties, PLoS ONE 16 (4) (2021) 1–11, doi:10.1371/journal.pone.0249271.
[32] P.L. Delamater, E.J. Street, T.F. Leslie, Y.T. Yang, K.H. Jacobsen, Complexity of the basic reproduction number (R0), Emerg. Infect. Dis. J. 25 (1) (2019), doi:10.3201/eid2501.171901.
[33] N.C. Bizet, A.C.M. de Oca, Modified SIR models for the evolution of COVID-19, Ciencias Matemáticas (2020) 73–87. https://reliefweb.int/sites/reliefweb.int/files/resources/20210622_Weekly_Epi_Update_45.pdf
[34] R. Subramanian, Q. He, M. Pascual, Quantifying asymptomatic infection and transmission of COVID-19 in New York city using observed cases, serology, and testing capacity, Proc. Natl. Acad. Sci. 118 (9) (2021), doi:10.1073/pnas.2019716118.
[35] I.F.-N. Hung, K.-C. Lung, E.Y.-K. Tso, R. Liu, T.W.-H. Chung, M.-Y. Chu, Y.-Y. Ng, J. Lo, J. Chan, A.R. Tam, H.-P. Shum, V. Chan, A.K.-L. Wu, K.-M. Sin, W.-S. Leung, W.-L. Law, D.C. Lung, S. Sin, P. Yeung, C.C.-Y. Yip, R.R. Zhang, A.Y.-F. Fung, E.Y.-W. Yan, K.-H. Leung, J.D. Ip, A.W.-H. Chu, W.-M. Chan, A.C.-K. Ng, R. Lee, K. Fung, A. Yeung, T.-C. Wu, J.W.-M. Chan, W.-W. Yan, W.-M. Chan, J.F.-W. Chan, A.K.-W. Lie, O.T.-Y. Tsang, V.C.-C. Cheng, T.-L. Que, C.-S. Lau, K.-H. Chan, K.K.-W. To, K.-Y. Yuen, Triple combination of interferon beta-1b, lopinavir-ritonavir, and ribavirin in the treatment of patients admitted to hospital with COVID-19: an open-label, randomised, phase 2 trial, The Lancet 395 (10238) (2020) 1695–1704, doi:10.1016/S0140-6736(20)31042-4. Publisher: Elsevier
[36] N. Hossein-Khannazer, B. Shokoohian, A. Shpichka, H.A. Aghdaei, P. Timashev, M. Vosough, Novel therapeutic approaches for treatment of COVID-19, J. Mol. Med. 98 (2020) 789–803, doi:10.1007/s00109-020-01927-6. Publisher: Springer